Published for SISSA by Springer

Received: *May 8, 2017*
Revised: *July 11, 2017*
Accepted: *July 12, 2017*
Published: *July 21, 2017*

# Studies of $Z\gamma$ production in association with a high-mass dijet system in $pp$ collisions at $\sqrt{s} = 8$ TeV with the ATLAS detector

## The ATLAS collaboration

*E-mail:* atlas.publications@cern.ch

Abstract: The production of a $Z$ boson and a photon in association with a high-mass dijet system is studied using 20.2 fb$^{-1}$ of proton-proton collision data at a centre-of-mass energy of $\sqrt{s} = 8$ TeV recorded with the ATLAS detector in 2012 at the Large Hadron Collider. Final states with a photon and a Z boson decaying into a pair of either electrons, muons, or neutrinos are analysed. Electroweak and total $pp \to Z\gamma jj$ cross-sections are extracted in two fiducial regions with different sensitivities to electroweak production processes. Quartic couplings of vector bosons are studied in regions of phase space with an enhanced contribution from pure electroweak production, sensitive to vector-boson scattering processes $VV \to Z\gamma$. No deviations from Standard Model predictions are observed and constraints are placed on anomalous couplings parameterized by higher-dimensional operators using effective field theory.

Keywords: Electroweak interaction, Hadron-Hadron scattering (experiments)

ArXiv ePrint: 1705.01966



https://doi.org/10.1007/JHEP07(2017)107

## Contents



JHEP07(2017)107

## 1 Introduction

The scattering of two vector bosons, $VV \to VV$ with $V = W/Z/\gamma$, is a key process for probing the $\mathrm{SU(2)_L} \times \mathrm{U(1)_Y}$ gauge symmetry of the electroweak theory that determines the self-couplings of the vector bosons. In particular, it is important to independently test the triple and quartic gauge-boson coupling strengths (TGCs and QGCs), since new phenomena could generate additional contributions to QGCs with respect to the Standard Model (SM) predictions [1–4], while not significantly affecting the TGCs [5].

Experimental information about QGCs is still limited. At the Large Hadron Collider (LHC), it can be deduced from studies of processes with either three bosons in the final state [6–10] or involving pure electroweak production of heavy dibosons [11–14]. In particular, the CMS experiment recently studied $Z\gamma$ [15] and $W\gamma$ [16] electroweak production

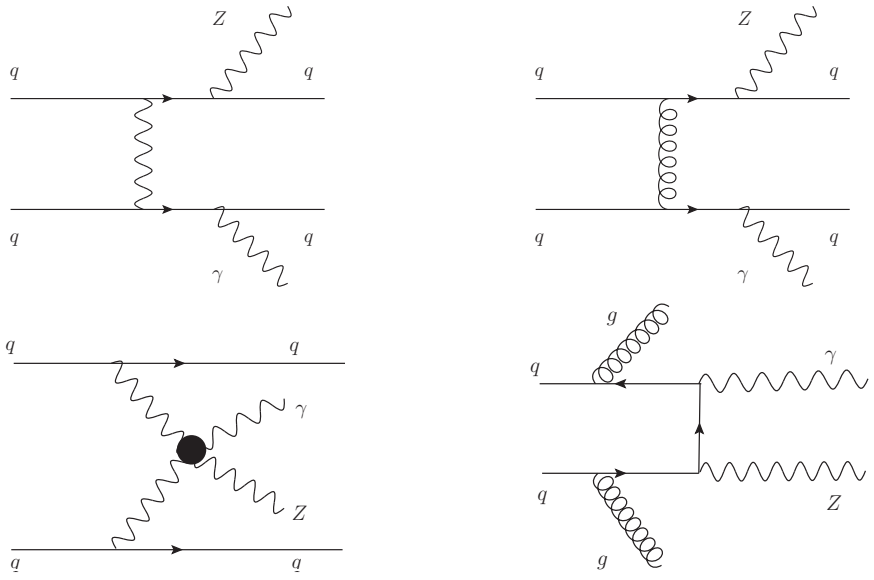


**Figure 1**. Feynman diagrams of electroweak $Z\gamma jj$ production involving VBS subprocesses (bottom left) or non-VBS subprocesses (top left) and of QCD $Z\gamma jj$ production with gluon exchange (top right) or radiation (bottom right).

and used these results to set limits on anomalous QGCs. Final states involving photons have higher rates than those involving only $W$ and $Z$ bosons identified via their leptonic decay modes.

The $Z\gamma jj$ electroweak (EWK) production ($qq \to qqZ\gamma$) — where $j$ represents a jet and $q$ a quark — contains processes with fourth-order electroweak coupling $\mathcal{O}(\alpha_{\text{em}}^4)$. These include vector-boson scattering (VBS) as well as non-VBS diagrams, e.g. when the $Z$ boson and the photon are radiated off the initial- or final- state quarks (figure 1, left). The VBS processes do not respect the electroweak gauge symmetry when taken in isolation and cannot be studied separately from other electroweak processes, due to large interference effects.

The same $Z\gamma jj$ final state can be produced by QCD-mediated processes — in the following simply called "QCD production" — with second-order electroweak coupling and second-order strong coupling $\mathcal{O}(\alpha_{\text{em}}^2\alpha_{\text{s}}^2)$ (figure 1, right). Such processes can involve radiated gluons in the initial and/or final state as well as quark scattering processes mediated by gluons. According to the SM, a small constructive interference occurs between production of QCD and EWK quark scattering.

Experimentally, $Z\gamma jj$ EWK processes are characterized by the production of two energetic hadronic jets with wide rapidity separation and large dijet invariant mass [17]. The vector-boson pair is typically produced more centrally than in non-EWK processes. These kinematic properties are exploited to select a phase-space region where the electroweak production is enhanced with respect to the QCD-mediated processes.

Previous measurements of inclusive and differential cross-sections of $Z\gamma$ production in proton-proton collisions at the centre-of-mass energy of 8 TeV performed by the ATLAS experiment [9] show good agreement (within 6%) between data and next-to-next-to-leading-order (NNLO) predictions.



JHEP07(2017)107

A study of $Z\gamma jj$ EWK production is made in a search region defined to maximize its expected significance. This corresponds to a phase-space region with a high-mass dijet system, a high-energy photon, and a $Z$ boson decaying into a pair of electrons or muons — in the following referred to as the "charged-lepton channel". The contribution from QCD production is constrained with data from a background-enriched control region, corresponding to events with lower dijet invariant mass. A fiducial cross-section is extracted and compared to SM predictions. The total $Z\gamma jj$ (EWK+QCD) production cross-section in both the search and control fiducial regions is also measured.

The $Z\gamma jj$ EWK production is also studied in events with high-transverse-energy ($E_{\mathrm{T}}$) photons, where an enhancement of the VBS cross-section is typically predicted by theories beyond the Standard Model. In this phase space region, a search for anomalies in the quartic $WWZ\gamma$ coupling along with the presence of $ZZZ\gamma$, $ZZ\gamma\gamma$ and $Z\gamma\gamma\gamma$ couplings — forbidden in the SM at tree level — is performed. Extensions of the SM Lagrangian are parameterized by higher-order operators in an effective field theory that modifies the boson couplings. The sensitivity of the search is improved by also considering events with the $Z$ boson decaying into neutrinos. The phase-space region optimized for anomalous QGC (aQGC) sensitivity is defined differently for the charged-lepton and neutrino channels. For the latter, since the $Z$ boson is experimentally invisible, extra requirements are included to suppress the relatively large backgrounds present in this channel.

The paper is organized as follows. A brief description of the ATLAS detector and the data set used in this analysis is given in section 2. The simulation of the contributing processes is summarized in section 3, while event reconstruction and selection is detailed in section 4. The determination of the backgrounds and event yields are discussed in section 5. The extraction of the cross-sections are described in section 6. Finally, a search for aQGCs using events with high-$E_{\mathrm{T}}$ photons is presented in section 7. Conclusions are drawn in section 8.

## 2 ATLAS detector and data

The ATLAS experiment [18] at the LHC is a multipurpose particle detector with a forward-backward symmetric cylindrical geometry and an almost $4\pi$ coverage in solid angle.[1] It consists of a tracking system called the inner detector (ID) surrounded by a thin superconducting solenoid providing a 2 T axial magnetic field, electromagnetic and hadronic calorimeters, and a muon spectrometer (MS). The ID covers the pseudorapidity range

[1]The ATLAS reference system is a Cartesian right-handed coordinate system with its origin at the nominal interaction point (IP) in the centre of the detector and the $z$-axis along the beam direction. The $x$-axis points from the IP to the centre of the LHC ring, and the $y$-axis points upwards. Cylindrical coordinates $(r, \phi)$ are used in the plane that is transverse to the beam direction, where $\phi$ describes the azimuthal angle around the beam pipe as measured from the positive $x$-axis. The rapidity ($y$) is defined as $y = 1/2 \times \ln[(E+p_z)/(E-p_z)]$ where $E$ ($p_z$) is the energy (the $z$-component of the momentum) of a particle. The pseudorapidity ($\eta$) is defined as $\eta = -\ln(\tan(\theta/2))$ where $\theta$ is the polar angle. The distance between two objects in the $\eta$–$\phi$ space is defined as $\Delta R \equiv \sqrt{(\eta_1-\eta_2)^2 + (\phi_1-\phi_2)^2}$ where $\eta_{1,2}$ ($\phi_{1,2}$) represents the pseudorapidities (azimuthal angles) of the two objects. The transverse momentum ($p_{\mathrm{T}}$) is defined relative to the beam axis and is calculated as $p_{\mathrm{T}} = p\sin\theta$ where $p$ is the momentum.



JHEP07(2017)107

$|\eta| < 2.5$. It consists of silicon pixel, silicon microstrip, and transition radiation tracking detectors. Within the region of $|\eta| < 3.2$, electromagnetic (EM) calorimetry is provided by high-granularity lead/liquid-argon (LAr) sampling calorimeters, with an additional thin LAr presampler covering $|\eta| < 1.8$ to correct for energy loss in material upstream of the calorimeters. A hadronic (steel/scintillator-tile) calorimeter covers the central pseudorapidity range ($|\eta| < 1.7$). The endcap and forward regions are instrumented with LAr calorimeters for both the EM and hadronic energy measurements up to $|\eta| = 4.9$. The MS surrounds the calorimeters and is based on three large air-core toroidal superconducting magnets with eight coils each. It includes a system of precision tracking chambers and fast detectors for triggering. A three-level trigger system is used to select events. The first-level trigger is implemented in hardware and uses a subset of the detector information to reduce the accepted rate to at most 75 kHz. This is followed by two software-based systems, called the high-level triggers, that together reduce the accepted event rate to 400 Hz on average, depending on the data-taking conditions.

The data set used in this analysis was obtained from proton-proton collisions recorded in 2012 by the ATLAS detector, when the LHC operated at $\sqrt{s} = 8$ TeV. The integrated luminosity of the data set used in this measurement is 20.2 fb$^{-1}$ with an uncertainty of 1.9% [19].

In the charged-lepton channel analysis, events are selected online by requiring the presence of either an isolated electron or muon candidate with a minimum transverse momentum ($p_{\mathrm{T}}$) of 24 GeV, or a pair of isolated electron candidates with $p_{\mathrm{T}} > 12$ GeV, or a pair of isolated muon candidates satisfying $p_{\mathrm{T}} > 18$ GeV and $p_{\mathrm{T}} > 8$ GeV for the leading and subleading muons. Trigger efficiencies are included in the overall reconstruction efficiency, and the uncertainties in the efficiency of these trigger selections were estimated using control samples in data and amount to 0.2% and 0.5% in the $e^+e^-\gamma jj$ and $\mu^+\mu^-\gamma jj$ channels, respectively.

In the neutrino channel, the events are selected online by requiring a photon candidate with $E_{\mathrm{T}} > 40$ GeV and missing transverse momentum greater than 60 GeV. Trigger efficiencies are included in the overall reconstruction efficiency, and the uncertainties in the efficiency of these trigger selections were estimated using control samples in data and amount to 2.0%.

## 3 Simulated samples and theory predictions

Monte Carlo (MC) event samples, using a full simulation [20] of the ATLAS detector by Geant 4 [21], are used to model the data, including contributions from the SM signal and expected backgrounds.

The individual $Z\gamma jj$ EWK and the $Z\gamma$ QCD (with up to three additional final-state partons) processes are modelled at leading order (LO) with the Sherpa event generator v1.4.5 [22]. The EWK-QCD interference contribution is predicted from MadGraph [23] to be less than 10% of the EWK cross-section in the search region — invariant mass of the two leading jets, $m_{jj}$, greater than 500 GeV— with a decreasing trend as a function of $m_{jj}$. This interference is treated as an uncertainty in the measurements, as discussed in section 6.1.



JHEP07(2017)107

Major background processes, such as $Z$+jets, $\gamma$+jets, $W$+jets, $WW$+jets, and $WZ$+jets are also modelled by the Sherpa event generator. These include up to five additional final-state partons at LO for the $V$+jets processes and up to three additional partons at LO for the $VV$+jets processes. All the Sherpa samples include parton showering (with the CKKW matching scheme [24, 25] scale set to 20 GeV), and fragmentation processes along with simulation of the underlying event. They are generated using the CT10 [26] parton distribution function (PDF) set.

Uncertainties in the Sherpa modelling of the $Z\gamma jj$ processes are estimated using 68% confidence-level PDF uncertainties, independent variations of renormalization and factorization scales by a factor of two and variations of the choice of CKKW scale (from 15 to 30 GeV).

Production of $t\bar{t}$ pairs is modelled by MC@NLO v4.06 [27, 28], interfaced to Herwig v6.520.2 for parton showering and fragmentation, and to Jimmy v4.31.3 [29] for underlying-event simulation. The $t\bar{t}\gamma$ production is modelled with MadGraph5_aMC@NLO v5.2.1.2 [23] and the CTEQ6L1 [30] PDF set, with parton showering, hadronization, and the underlying event modelled by Pythia v8.183 [31]. The cross-section is computed at next-to-leading-order (NLO) according to ref. [32].

Some of the systematic uncertainties of the $Z$+jets background estimate, which is extracted from data, are estimated using $Z$+jets NLO Powheg-Box v1.0 and LO Alpgen v2.1.4 (with up to five additional final-state partons) generated events. These samples are interfaced with Pythia v8.175 and Herwig v6.520.2 + Jimmy v4.31.3 respectively for the modelling of the parton shower, hadronization and underlying event.

Multiple proton-proton collisions (pile-up), corresponding to the conditions observed during the 2012 run, are added to each MC sample. This pile-up is simulated using Pythia v8.165 [31] with parameter values set according to the A2 tune [33] and the MSTW2008LO PDF set [34]. MC events are then reweighted so that the pile-up conditions in the simulation match those observed in the data.

The SM cross-section predictions for both the $Z\gamma jj$ EWK and QCD processes with exactly two additional final-state partons are calculated at NLO precision in $\alpha_s$ using the Vbfnlo event generator v2.7.1 [35–37]. All spin correlations and finite-width effects are included in the matrix-element calculation, and for EWK production all resonant and non-resonant $t$-channel exchange contributions giving rise to a specific leptonic final state are considered. The CT10 PDF set is used for both EWK and QCD production as well as for the underlying-event generation and tune. These samples are generated separately (i.e. the interference between EWK and QCD is not taken into account in the modelling). A photon isolation requirement to remove the contributions from partons collinear to the photon is also included in the calculation. The uncertainty in these predictions due to the PDF and the choice of renormalization/factorization scale ranges from 4% to 10% depending on the processes and phase-space regions.



JHEP07(2017)107

## 4 Event reconstruction and selection

### 4.1 Event reconstruction

Events are required to have a reconstructed primary vertex formed by at least two tracks with $p_{\mathrm{T}} > 400\,\mathrm{MeV}$ and $|\eta| < 2.5$. If more than one primary vertex is found, the one with the largest sum of the $p_{\mathrm{T}}^2$ of the associated tracks is chosen as the hard-interaction vertex.

Electron candidates, reconstructed by matching an energy deposit in the calorimeter to a track in the ID, are required to have $E_{\mathrm{T}} > 25\,\mathrm{GeV}$ and $|\eta| < 2.47$. In addition, they must satisfy a set of "Loose" [38] identification criteria based on a combination of shower shape information from the EM calorimeter and tracking information from the ID, corresponding to an average selection efficiency of about 93%. The electron tracks are required to have longitudinal impact parameter smaller than 0.5 mm with respect to the hard-interaction vertex, and the absolute value of the transverse impact parameter with respect to the primary vertex less than six times its measured uncertainty, to reduce semi-leptonic heavy flavor decay backgrounds. Electron candidates are also required to be isolated. This is achieved by requiring the sum of the transverse momenta of ID tracks associated with the primary vertex in a cone of size $\Delta R = 0.3$ around the electron direction, excluding the electron track, to be less than 10% of the transverse energy of the electron candidate itself. Uncertainties in the electron selection arise from: identification [38] and impact parameter selection variations; changes in the isolation definition; and uncertainties in the electron energy scale and resolution [39].

Muon candidates are reconstructed by combining tracks in the ID with tracks in the MS and are required to have $p_{\mathrm{T}} > 25\,\mathrm{GeV}$ and $|\eta| < 2.5$. The ID tracks associated with these muons must satisfy several quality selection criteria [40]. The same requirement on the longitudinal impact parameter as for the electron track is also imposed on the combined muon track. The overall selection efficiency of the muon identification is about 97%. Muon candidates are required to be isolated using the same criteria as for electrons, but using a cone of size $\Delta R = 0.2$. Uncertainties in the muon selection are derived from uncertainties in the muon momentum scale and resolution [40], and by varying the selection criteria on the muon track quality, impact parameter or isolation.

Photon reconstruction and identification criteria are based on the expected shapes of showers developing in the electromagnetic calorimeter, as described in ref. [41]. Photons must be within the fiducial volume of the central calorimeter ($|\eta| < 2.37$) and outside the transition region between the barrel and endcap calorimeters ($1.37 < |\eta| < 1.52$). The sum of the transverse energies of topological clusters reconstructed in the electromagnetic and hadronic calorimeters in a cone of size $\Delta R = 0.4$ around the photon candidate, from which the energy of the photon cluster together with the median energy density of the event times the cone area are subtracted [42, 43], is required to be less than 6 GeV. Photon candidates are rejected if they are not well separated from the previously selected leptons, i.e. if $\Delta R(\gamma, \ell) < 0.4$. The overall efficiency of this photon selection on $Z\gamma jj$ EWK events is about 37% (96%) for photons with $E_{\mathrm{T}}^{\gamma} > 15$ (150) GeV. Uncertainties in the photon selection come from: variations in the reconstruction and identification criteria [41]; changes in the isolation requirements; and uncertainties in the photon energy scale and resolution [39].



JHEP07(2017)107

Jets are reconstructed from clusters of energy in the calorimeter using the anti-$k_t$ algorithm [44] with radius parameter $R = 0.4$. Jet energies are calibrated using energy- and $\eta$-dependent correction factors derived using MC simulation and validated by studying collision data [45]. Jets are considered if they have $p_{\mathrm{T}} > 30\,\mathrm{GeV}$ and $|\eta| < 4.5$. To remove jets originating from additional collisions in the same bunch crossing, at least 50% of the summed scalar $p_{\mathrm{T}}$ of the tracks within a cone of size $\Delta R = 0.4$ around the jet axis must originate from the hard-interaction vertex. This criterion is applied only to jets with $p_{\mathrm{T}} < 50\,\mathrm{GeV}$ and $|\eta| < 2.4$ [46]. Jet candidates are rejected if they are not well separated from the previously selected leptons and photons, i.e if $\Delta R(j, \ell) < 0.3$ or $\Delta R(j, \gamma) < 0.4$. Systematic effects in jet reconstruction lead primarily to uncertainties in the jet energy scale (JES) and resolution (JER) and are described in ref. [45].

The determination of the two-dimensional missing transverse-momentum vector, $\vec{p}_{\mathrm{T}}^{\,\mathrm{miss}}$, is based on the measurement of all topological clusters in the calorimeter and muon tracks reconstructed in the ID and MS [47]. Calorimeter cells associated with reconstructed objects, such as electrons, photons, $\tau \to$ hadrons $+ \nu$ decays, and jets, are calibrated at their own energy scale, whereas calorimeter cells not associated with any object are calibrated at the electromagnetic energy scale. The magnitude of this vector is denoted by $E_{\mathrm{T}}^{\mathrm{miss}}$. Uncertainties in the measurement of $E_{\mathrm{T}}^{\mathrm{miss}}$ are derived from uncertainties in measurements of the contributing objects.

### 4.2 Selection of $\ell^+\ell^-\gamma jj$ events

In the charged-lepton channel, $\ell^+\ell^-\gamma jj$ events are required to have one photon candidate with $E_{\mathrm{T}}^{\gamma} > 15\,\mathrm{GeV}$, a pair of opposite-sign (OS), same-flavour leptons (electrons or muons) and at least two reconstructed jets.

The invariant mass of the two leptons, $m_{\ell\ell}$, must be at least 40 GeV. The sum of the dilepton mass and the three-body $\ell\ell\gamma$ invariant mass is required to be larger than 182 GeV, which is approximately twice the $Z$ boson mass. This requirement ensures that the three-body invariant mass is larger than the $Z$ boson mass, thus suppressing the cases where the $Z$ boson decay products radiate a photon.

The event topology of $Z\gamma jj$ EWK production is characterized by the presence of two bosons in the central region and two jets with large rapidity difference and large dijet mass. Different phase-space regions are considered based on $m_{jj}$. The inclusive region is defined by events with no requirement on the dijet invariant mass, the control region (CR) is defined by events with $150 < m_{jj} < 500\,\mathrm{GeV}$, and the search region (SR) is defined by requiring $m_{jj} > 500\,\mathrm{GeV}$. The requirement of $m_{jj} > 150\,\mathrm{GeV}$ suppresses the background process of $Z\gamma + W(\to jj)$ triboson to negligible levels. The search region definition is optimized for the best expected significance for the $Z\gamma jj$ EWK process, given the amount of data.

Finally, the fiducial phase-space region optimized for sensitivity to anomalous quartic couplings (the "aQGC region"), is defined by requiring events in the search region to have a photon with $E_{\mathrm{T}}^{\gamma} > 250\,\mathrm{GeV}$. The expected numbers of $Z\gamma jj$ EWK events in the search and aQGC regions are $22.8 \pm 1.5$ and $0.41 \pm 0.04$, respectively.



JHEP07(2017)107

A centrality observable $\zeta$ is defined to quantify the relative position in pseudorapidity of a particle or system of particles with respect to the two leading jets ($j_1$ and $j_2$):

$$\zeta \equiv \left| \frac{\eta - \bar{\eta}_{jj}}{\Delta\eta_{jj}} \right| \quad \text{with} \quad \bar{\eta}_{jj} = \frac{\eta_{j_1} + \eta_{j_2}}{2}, \quad \Delta\eta_{jj} = \eta_{j_1} - \eta_{j_2}, \tag{4.1}$$

where $\eta$ is the pseudorapidity of the physics object. The centrality of the $Z\gamma$ system, $\zeta_{Z\gamma}$, allows discrimination between $Z\gamma jj$ EWK and QCD production, with the former contributing more at low values of $\zeta_{Z\gamma}$. However, to maximize the statistical power of the sample, no explicit $\zeta_{Z\gamma}$ requirement is implemented, but rather the full $\zeta_{Z\gamma}$ distribution is used to extract the $Z\gamma jj$ cross-sections, as detailed in section 6.

### 4.3 Selection of $\nu\bar{\nu}\gamma jj$ events

In the neutrino channel analysis, the $Z$ boson signature is high missing transverse momemtum from the undetected neutrino pair. Therefore, the $\nu\bar{\nu}\gamma jj$ candidate events are required to have $E_{\mathrm{T}}^{\mathrm{miss}} > 100\,\mathrm{GeV}$, which corresponds to a relative $Z\gamma jj$ EWK efficiency of 85%, along with the presence of a candidate photon with $E_{\mathrm{T}}^{\gamma} > 150\,\mathrm{GeV}$ and at least two jets.

A lepton veto requirement (on the presence of electrons or muons as defined above) is applied to reduce the large contribution from $W(\ell\nu)\gamma$+jets events. This requirement is almost 100% efficient for $Z\gamma jj$ events.

Requirements on event topology are introduced to suppress the large background from $\gamma$+jets (where $\vec{p}_{\mathrm{T}}^{\,\mathrm{miss}}$ is usually collinear with jets) and $W(e\nu)$+jets events. This is achieved by applying a set of angular selection criteria: the azimuthal difference between $\vec{p}_{\mathrm{T}}^{\,\mathrm{miss}}$ and the total transverse momentum of the photon and the two jets should be larger than $3\pi/4$, $(\Delta\phi(\vec{p}_{\mathrm{T}}^{\,\mathrm{miss}}, \gamma jj) > 3\pi/4)$; the azimuthal difference between $\vec{p}_{\mathrm{T}}^{\,\mathrm{miss}}$ and the photon should be larger than $\pi/2$, $(\Delta\phi(\vec{p}_{\mathrm{T}}^{\,\mathrm{miss}}, \gamma) > \pi/2)$; and the azimuthal difference between $\vec{p}_{\mathrm{T}}^{\,\mathrm{miss}}$ and each of the two jets should be larger than 1, $(\Delta\phi(\vec{p}_{\mathrm{T}}^{\,\mathrm{miss}}, j) > 1)$. Overall, these angular separation requirements suppress the background by a factor of 40, with a relative $Z\gamma jj$ EWK efficiency of 33%.

To enhance the $Z\gamma jj$ EWK production and maximize the sensitivity to aQGC, further event topology selections are applied: the absolute rapidity difference between the two jets is required to be greater than 2.5 ($|\Delta y_{jj}| > 2.5$), the photon centrality must be smaller than 0.3 ($\zeta_{\gamma} < 0.3$), the $p_{\mathrm{T}}^{\mathrm{balance}}$ of the $\nu\bar{\nu}\gamma jj$ object, defined as

$$p_{\mathrm{T}}^{\mathrm{balance}} \equiv \frac{|\vec{p}_{\mathrm{T}}^{\,\mathrm{miss}} + \vec{p}_{\mathrm{T}}^{\,\gamma} + \vec{p}_{\mathrm{T}}^{\,j_1} + \vec{p}_{\mathrm{T}}^{\,j_2}|}{E_{\mathrm{T}}^{\mathrm{miss}} + |\vec{p}_{\mathrm{T}}^{\,\gamma}| + |\vec{p}_{\mathrm{T}}^{\,j_1}| + |\vec{p}_{\mathrm{T}}^{\,j_2}|}, \tag{4.2}$$

must be smaller than 0.1, and the dijet invariant mass must be greater than 600 GeV. These event topology requirements further reduce the background by a factor of 80, with a relative $Z\gamma jj$ EWK efficiency of 20%. The expected number of $Z\gamma jj$ EWK events after all the selection requirements is $0.65 \pm 0.05$.



JHEP07(2017)107

## 5 Background estimate and event yields

### 5.1 Backgrounds in the charged-lepton channels

The main background to the $Z\gamma jj$ production processes comes from the misidentification of hadronic jets as photons (jets faking photons) in $Z$+jets events. This background is not well modelled by the MC simulation. It is estimated with data using the same two-dimensional sideband method [43] used in the inclusive $Z\gamma$ cross-section measurement [9]. The method is based on control regions populated by events satisfying all selection criteria but with the candidate photon failing to satisfy some of the identification criteria and/or the isolation requirement.

Due to the very limited number of events in the search and control regions, the background contribution from $Z$+jets events is estimated in an enlarged phase-space region, relaxing the dijet mass requirement to $m_{jj} > 100\,\text{GeV}$. This is the most stringent requirement on $m_{jj}$ where the uncertainty on the background estimated is still dominated by systematic errors. The extrapolation of the background estimate to the search and control regions relies on the observation that the shape of the $m_{jj}$ distribution of $Z$+jets background events (i.e. with one jet faking a photon) in both the Powheg and Alpgen MC samples is similar to the $m_{jj}$ distribution of $Z\gamma$ events in Sherpa MC samples, for $m_{jj} > 100\,\text{GeV}$. Therefore, the ratio of $Z$+jets to $Z\gamma$ contribution can be considered the same in the enlarged phase-space region as in the search and control regions.

In the enlarged phase-space region ($m_{jj} > 100\,\text{GeV}$), the contribution from $Z$+jets events is estimated with data to be $(23 \pm 6)\%$ of $Z\gamma$ events. The uncertainty is dominated by the systematic uncertainty due to the correlation between photon identification and isolation requirements. This correlation is calculated from MC simulation and the large systematic uncertainty reflects the different responses from Sherpa , Pythia and Alpgen modelling. Other systematic uncertainties related to control region definition, signal contamination in control regions, and $m_{jj}$ shape difference between $Z$+jets and $Z\gamma$ are found to be negligible compared to the normalization uncertainty and are neglected.

Besides the $Z$+jets process, other background contributions are from $WZ$+jets events, with a misidentification of an electron as a photon, and $t\bar{t}\gamma$ events, with the photon emitted from initial-state partons or final-state leptons. The yields of these two processes are estimated from MC simulation with an uncertainty determined by the measured cross-sections uncertainty.

### 5.2 Backgrounds in the neutrino channel

For the neutrino channel, background events mainly arise from processes having final states similar to the signal, from events with jets or electrons misidentified as photons, and from events with high fake $E_{\text{T}}^{\text{miss}}$ (i.e. due to mismeasurement of hadronic energy deposits rather than the presence of neutrinos in the events). The main background processes are $W(\ell\nu)\gamma$+jets, $Z(\nu\bar{\nu})$+jets, $\gamma$+jets and $W(e\nu)$+jets accounting for approximately 59%, 15%, 7%, and 5% of the total background, respectively.

The dominant background is $W(\ell\nu)\gamma$+jets production, where the lepton is either not reconstructed or not identified, making the lepton veto requirement ineffective. In particu-



JHEP07(2017)107

lar, $W(\tau\nu)\gamma$+jets events, with $\tau \to$ hadrons$+\nu$ decays, provide a considerable contribution to this background. The $W\gamma$+jets background, which includes both the QCD and EWK components, is estimated using the Sherpa MC samples. The normalization is determined with data. The MC yield of $W(\ell\nu)\gamma$+jets events is corrected by constructing a data sample from events passing the $\nu\bar{\nu}\gamma jj$ inclusive selection and requiring exactly one charged lepton in the event (instead of vetoing them). The fraction of $W\gamma$ events in this sample is about 80%, and these data events (after subtracting non-$W\gamma$ contributions from MC estimates) are used to determine a correction factor for the MC yield of the $W\gamma$+jets sample, which is found to be 1.06. The difference between the background estimates extracted from Sherpa and Alpgen MC samples is the dominant systematic uncertainty in the $W\gamma$+jets background prediction, corresponding to a relative uncertainty of 41%.

The second largest source of background comes from $Z(\nu\bar{\nu})$+jets, where a jet is misidentified as an energetic photon. The contribution of this background is estimated with the same two-dimensional sideband method used to determine the $Z$+jets contribution in the charged-lepton channel. In this case, however, the background estimate is performed directly in the phase-space region of interest. The statistical uncertainty of 50% is significantly larger than the systematic uncertainty, which amounts to 20%.

Another important source of background is the production of $\gamma$+jets events with fake $E_{\mathrm{T}}^{\mathrm{miss}}$. This background is estimated with data, again using a two-dimensional sideband method. The control regions are composed of events with low $E_{\mathrm{T}}^{\mathrm{miss}}$ and/or with low values of $\Delta\phi(\vec{p}_{\mathrm{T}}^{\,\mathrm{miss}}, j)$. Due to the limited size of the data sample, the background estimate is performed with a relaxed energy requirement on the photon ($E_{\mathrm{T}}^{\gamma} > 45\,\mathrm{GeV}$) and then extrapolated to the phase-space region of interest using MC samples. The difference between the extrapolation results obtained with Sherpa and Alpgen samples (∼40%) is the dominant uncertainty for this background.

The sizeable production of $W(e\nu)$+jets is also a source of background when the electron is misidentified as a high-energy photon. To estimate this background, first the fake rate of $e \to \gamma$ misidentification is extracted from data using electrons from $Z \to ee$ events. Then the $W(e\nu)$+jets background contribution is estimated by applying this fake rate to events passing the full event selection but choosing a high-energy electron instead of a photon. The main uncertainty comes from the limited size of the control sample and equals 43%.

The background contribution from $Z(\tau\tau)\gamma$ is also estimated with MC samples and found to be less than 1%.

### 5.3 Expected and observed event yields

Table 1 summarizes the event yield for the charged-lepton channel, including details from the various signal and background processes. Three different phase-space regions are presented: inclusive $Z\gamma + \geq 2$ jets selection, CR and SR. A breakdown of the sources of systematic uncertainty in the CR and SR is given in table 2. Table 3 summarizes the event yield for both the charged-lepton and neutrino channels in the aQGC region with systematic uncertainties summarized in table 4. In the aQGC region, relative uncertainties in the yield in the charged-lepton channel are the same as those in the SR except for that



JHEP07(2017)107

| | Inclusive region $Z(\ell^+\ell^-)\gamma + \geq 2$ jets | | Control region $150 < m_{jj} < 500$ GeV | | Search region $m_{jj} > 500$ GeV | |
|---|---|---|---|---|---|---|
| | $e^+e^-\gamma jj$ | $\mu^+\mu^-\gamma jj$ | $e^+e^-\gamma jj$ | $\mu^+\mu^-\gamma jj$ | $e^+e^-\gamma jj$ | $\mu^+\mu^-\gamma jj$ |
| Data | 781 | 949 | 362 | 421 | 58 | 72 |
| $Z$+jets bkg. | $134 \pm 36$ | $154 \pm 42$ | $57 \pm 16$ | $67 \pm 18$ | $8.5 \pm 2.5$ | $9.4 \pm 2.7$ |
| Other bkg. ($t\bar{t}\gamma$, $WZ$) | $88 \pm 17$ | $91 \pm 18$ | $47 \pm 9$ | $46 \pm 9$ | $5.8 \pm 1.1$ | $5.0 \pm 1.0$ |
| $N_{\text{data}} - N_{\text{bkg}}$ | $559 \pm 46$ | $704 \pm 53$ | $258 \pm 24$ | $308 \pm 27$ | $44 \pm 7$ | $58 \pm 8$ |
| $N_{Z\gamma\ \text{QCD}}$ (SHERPA MC) | $583 \pm 41$ | $671 \pm 47$ | $249 \pm 24$ | $290 \pm 26$ | $37 \pm 5$ | $41 \pm 5$ |
| $N_{Z\gamma\ \text{EWK}}$ (SHERPA MC) | $25.4 \pm 1.5$ | $27.3 \pm 1.7$ | $8.6 \pm 0.6$ | $9.3 \pm 0.6$ | $11.2 \pm 0.8$ | $11.6 \pm 0.7$ |
| $N_{Z\gamma}$ (SHERPA MC) | $608 \pm 42$ | $698 \pm 49$ | $258 \pm 25$ | $299 \pm 27$ | $48 \pm 6$ | $53 \pm 6$ |

**Table 1**. Summary of events observed in data and estimated composition for the $Z(e^+e^-)\gamma jj$ and $Z(\mu^+\mu^-)\gamma jj$ production processes. The $Z$+jets contribution in this table is taken as a fixed fraction, $(23 \pm 6)\%$, of $N_{Z\gamma\ \text{QCD}}$. The last line corresponds to the sum of the two previous lines ($N_{Z\gamma\ \text{QCD}}$ + $N_{Z\gamma\ \text{EWK}}$). The uncertainties correspond to the statistical and systematic uncertainties added in quadrature.

| Source of uncertainty | EWK yield [%] CR | EWK yield [%] SR | QCD yield [%] CR | QCD yield [%] SR | Bkg. yield [%] CR | Bkg. yield [%] SR |
|---|---|---|---|---|---|---|
| Trigger | | | 0.2 (0.4) | | | |
| Pile-up | | | 0.6 | | | |
| Lepton selection | | | 3.8 (2.3) | | | |
| Photon selection | | | 1.6 | | | |
| Jet reconstruction | 1.1 | 2.5 | 5.0 | 12 | 4.9 | 12 |
| Bkg. 2D sideband | - | - | - | - | 26 | 26 |
| Total experimental | 4.3 (3.1) | 4.9 (3.8) | 6.5 (5.8) | 13 (12) | 27 (27) | 29 (29) |
| Theory | 5.2 | 8.7 | 5.6 | 3.8 | 5.6 | 3.8 |

**Table 2**. Summary of the dominant experimental systematic uncertainties in the event yield in the CR and SR, for the electron (muon when different) channel and for the signal and main background components.

arising from photon selection. This component is larger due to the higher value required for the photon transverse energy in the aQGC region.

Figure 2 displays the transverse energy of the photon after various selection requirements (inclusive selection, control and search regions); figure 3 shows the numbers of selected jets in the control and search regions; figure 4 shows the distribution of the dijet mass for the inclusive selection; and finally figure 5 displays the distributions of $\zeta_{Z\gamma}$ in the inclusive, control and search regions. Corresponding kinematic distributions for the neutrino channel are shown in figure 6. The SHERPA MC prediction is found to describe the data well for all these variables and in all phase-space regions.



JHEP07(2017)107

| | aQGC region | |
|---|---|---|
| | $m_{jj} > 500\,\text{GeV}$ | $m_{jj} > 600\,\text{GeV}$ |
| | $E_{\text{T}}^{\gamma} > 250\,\text{GeV}$ | $E_{\text{T}}^{\gamma} > 150\,\text{GeV}$ |
| | $\ell^+\ell^-\gamma jj$ | $\nu\bar{\nu}\gamma jj$ |
| Data | 2 | 4 |
| $Z$+jets background | $0.28 \pm 0.08$ | $0.3 \pm 0.2$ |
| $W(\ell\nu)\gamma$+jets background | - | $1.1 \pm 0.5$ |
| $\gamma$+jets background | - | $0.13 \pm 0.08$ |
| $W(e\nu)$+jets background | - | $0.09 \pm 0.04$ |
| $t\bar{t}\gamma$, $WZ$ background | $0.02 \pm 0.01$ | - |
| $N_{\text{data}} - N_{\text{bkg}}$ | $1.7 \pm 1.4$ | $2.4 \pm 2.0$ |
| $N_{Z\gamma\ \text{QCD}}$ (Sherpa MC) | $1.2 \pm 0.4$ | $0.29 \pm 0.07$ |
| $N_{Z\gamma\ \text{EWK}}$ (Sherpa MC) | $0.41 \pm 0.04$ | $0.65 \pm 0.05$ |
| $N_{Z\gamma}$ (Sherpa MC) | $1.6 \pm 0.4$ | $0.9 \pm 0.1$ |

**Table 3**. Summary of events observed in data and estimated composition of the background for the $Z(\ell\ell)\gamma jj$ and $Z(\nu\bar{\nu})\gamma jj$ production processes in the aQGC region. The last line corresponds to the sum of the two previous lines ($N_{Z\gamma\ \text{QCD}} + N_{Z\gamma\ \text{EWK}}$). The quoted uncertainty corresponds to the total statistical plus systematic uncertainty added in quadrature.

| Source of | EWK yield [%] | | QCD yield [%] | |
|---|---|---|---|---|
| uncertainty | $\ell^+\ell^-$ channel | $\nu\bar{\nu}$ channel | $\ell^+\ell^-$ channel | $\nu\bar{\nu}$ channel |
| Trigger | 0.2 (0.4) | 2 | 0.2 (0.4) | 2 |
| Pile-up | | 0.6 | | |
| Lepton selection | 3.8 (2.3) | - | 3.8 (2.3) | - |
| $E_{\text{T}}^{\text{miss}}$ reconstruction | - | 0.4 | - | 0.4 |
| Photon selection | 6.5 | 3.3 | 6.5 | 3.3 |
| Jet reconstruction | 2.5 | 3.2 | 12 | 3.2 |
| Total experimental | 8.0 (7.4) | 5.1 | 13 | 5.1 |
| Theory | 8.7 | 4.1 | 3.8 | 4.1 |

**Table 4**. Summary of the main relative uncertainties in the MC-based EWK and QCD yields for the electron (muon when different) and neutrino channels in the aQGC region. The uncertainties in the $Z$+jets, $W(\ell\nu)\gamma$+jets, $\gamma$+jets, and $W(e\nu)$+jets yields, estimated with data, are detailed in the text.

JHEP07(2017)107

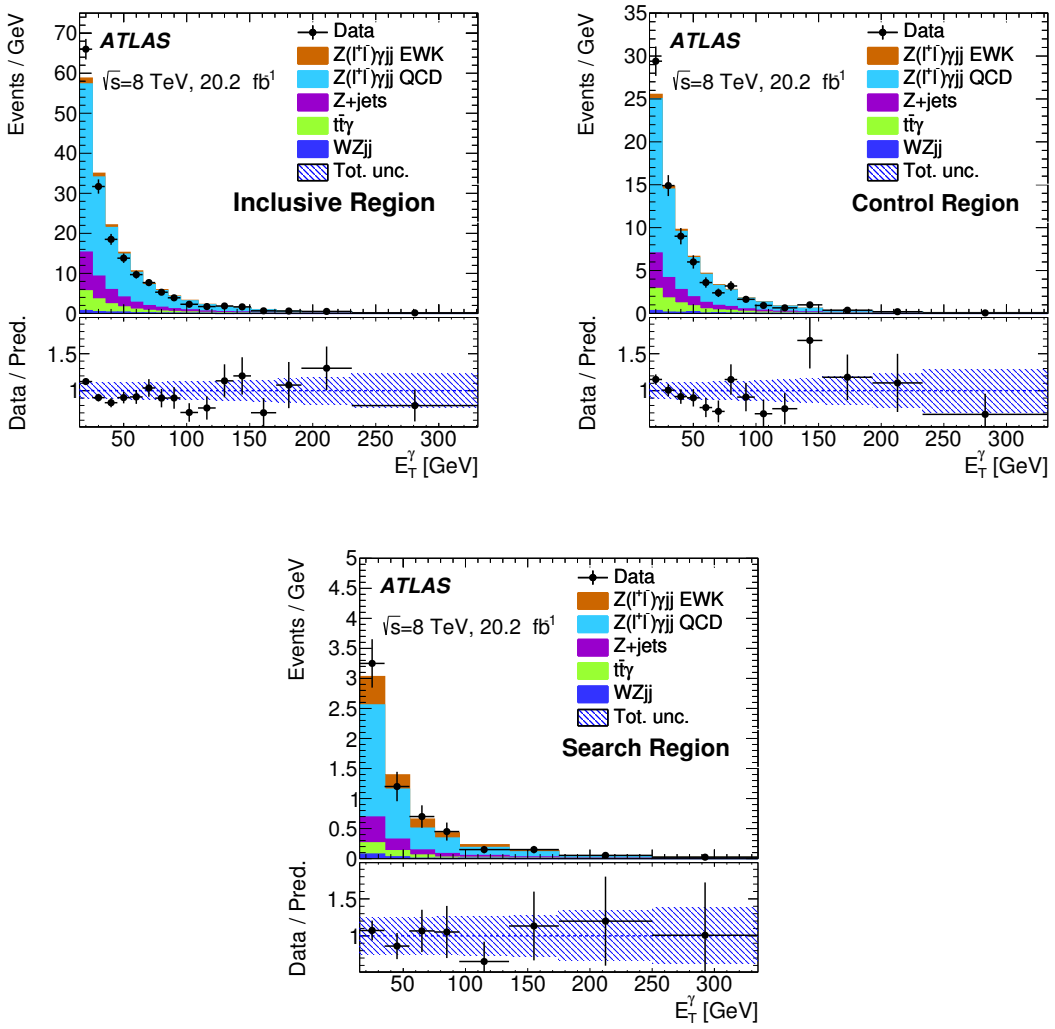


**Figure 2**. Distributions of the photon transverse energy for the electron and muon channels added together in the inclusive region (top left), in the control region (top right) and in the search region (bottom), for the data (black points), and for the signal process and various background components (coloured templates) before any fit is done. The ratio of the data to the sum of all pre-fit expected contributions ("Pred.") is shown below each histogram. The hatched blue band shows the systematic and statistical uncertainty added in quadrature ("Tot. unc.") in the signal and background prediction, while the error bars on the data points represent the statistical uncertainty of the data set. The number of events in each bin is divided by the bin width. The last bin also includes events beyond the range shown.

JHEP07(2017)107

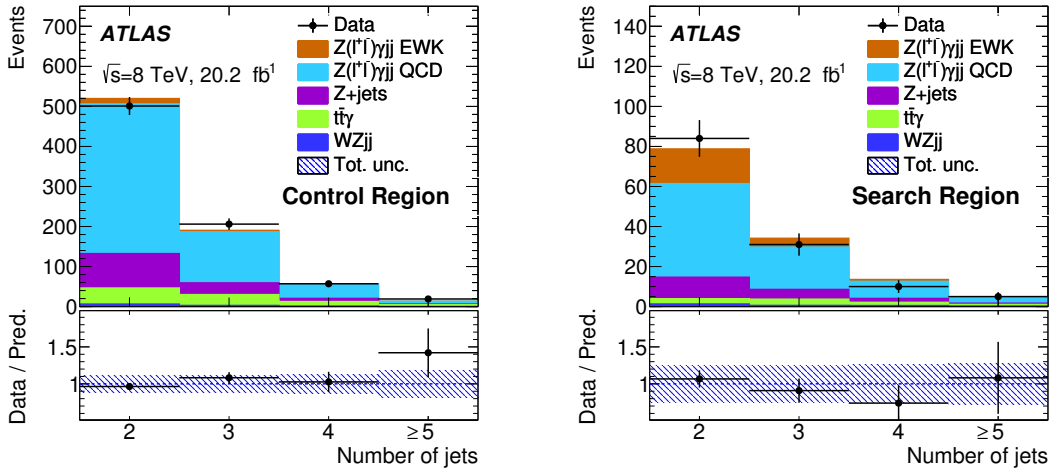


**Figure 3**. Distributions of the number of jets passing the selection for the electron and muon channels added together in the control region (left) and in the search region (right), for the data (black points), and for the signal process and various background components (coloured templates) before any fit is done. The ratio of the data to the sum of all pre-fit expected contributions ("Pred.") is shown below each histogram. The hatched blue band shows the systematic and statistical uncertainty added in quadrature ("Tot. unc.") in the signal and background prediction, while the error bars on the data points represent the statistical uncertainty of the data set. The last bin also includes events beyond the range shown.

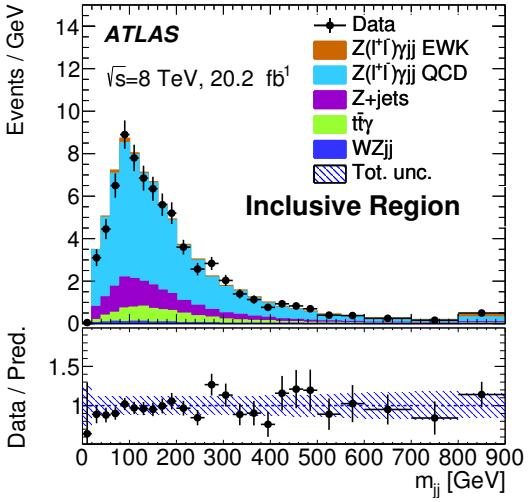


**Figure 4**. Distributions of the dijet invariant mass of the two leading jets for the electron and muon channels added together in the inclusive region, for the data (black points), and for the signal process and various background components (coloured templates) before any fit is done. The ratio of the data to the sum of all pre-fit expected contributions ("Pred.") is shown below the histogram. The hatched blue band shows the systematic and statistical uncertainty added in quadrature ("Tot. unc.") in the signal and background prediction, while the error bars on the data points represent the statistical uncertainty of the data set. The number of events in each bin is divided by the bin width. The last bin also includes events beyond the range shown.

JHEP07(2017)107

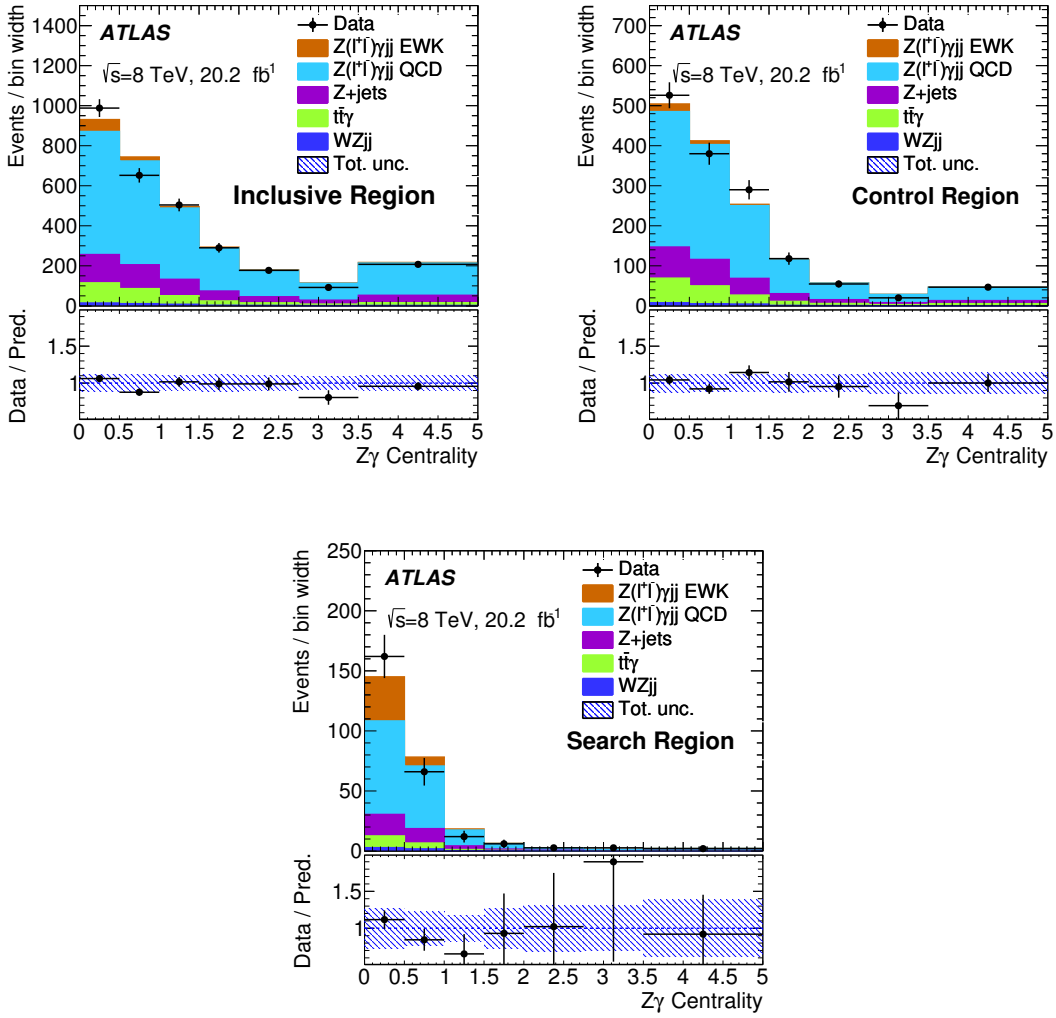


**Figure 5**. Distributions of centrality of the $Z\gamma$ system, $\zeta_{Z\gamma}$, for the electron and muon channels added together in the inclusive region (top left), in the control region (top right) and in the search region (bottom), for the data (black points), and for the signal process and various background components (coloured templates) before any fit is done. The ratio of the data to the sum of all pre-fit expected contribution ("Pred.") is shown below each histogram. The hatched blue band shows the systematic and statistical uncertainty added in quadrature ("Tot. unc.") in the signal and background prediction, while the error bars on the data points represent the statistical uncertainty of the data set. The number of events in each bin is divided by the bin width. The last bin also includes events beyond the range shown.

JHEP07(2017)107

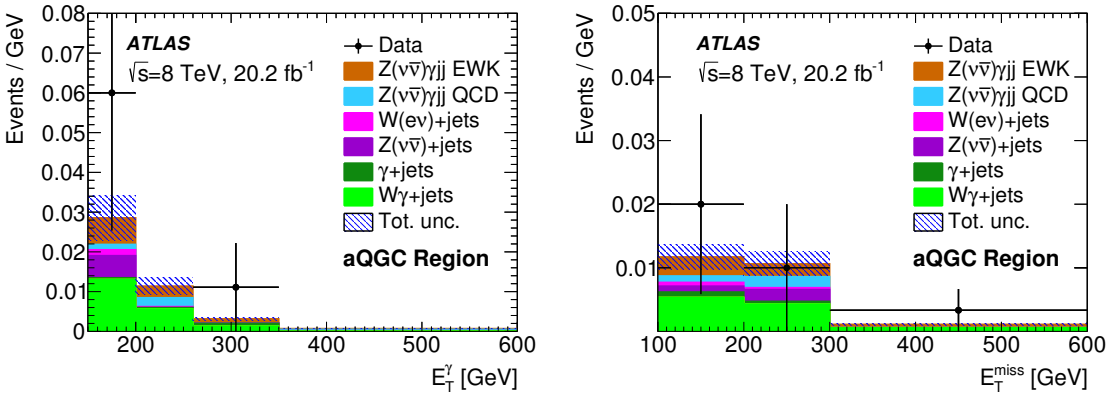


**Figure 6**. Distributions of the photon transverse energy $E_{\mathrm{T}}^{\gamma}$ (left) and $E_{\mathrm{T}}^{\mathrm{miss}}$ (right) for the neutrino channel in the aQGC region with $E_{\mathrm{T}}^{\gamma} \geq 150\,\mathrm{GeV}$ for the data (black points), and for the signal process and various background components (coloured templates). The hatched blue band shows the systematic and statistical uncertainty added in quadrature ("Tot. unc.") in the signal and background prediction, while the error bars on the data points represent the statistical uncertainty of the data set. The number of events in each bin is divided by the bin width. The last bin also includes events beyond the range shown.

## 6 Fiducial $Z\gamma jj$ cross-section measurements in the charged-lepton channel

In this section, the extraction of the $Z\gamma jj$ EWK production cross-section in the SR of the charged-lepton channel along with the $Z\gamma jj$ total (EWK+QCD) production cross-section in both the search and control regions of the charged-lepton channel is reported. Given the very limited number of signal events expected after the $\nu\bar{\nu}\gamma jj$ selection, that topology is only used in the search for anomalous quartic couplings described in section 7.

Fiducial regions are defined at the particle level, using stable particles — those with proper lifetime longer than 10 ps — before their interaction with the detector. Prompt lepton four-momenta — not from hadron or $\tau$ decays — are obtained through a four-vector sum of leptons with radiated photons within a cone of radius $\Delta R = 0.1$ around the leptons ("dressed leptons"). Jets are reconstructed with the anti-$k_t$ jet reconstruction algorithm with radius parameter $R = 0.4$ using stable particles, excluding muons and neutrinos. The photon isolation energy is taken as the energy of the jet matching the photon ($\Delta R(j,\gamma) < 0.3$), with the photon energy subtracted. These fiducial phase-space regions where the measurements are performed are defined to be as close as possible to the experimental phase-space regions, corresponding to the reconstructed-event selection described in section 4. This minimizes the extrapolation to the particle-level phase space by the MC simulation. Table 5 summarizes the selection that are applied to obtain the various fiducial regions. The fraction of events in the SR fiducial region passing the reconstructed event selection is about 94% for the charged-lepton channel.

The parton-level selection, used to calculate the predicted cross-section with the VBFNLO MC event generator, is basically identical to the particle-level selection described above, with jet selection requirements directly applied to the outgoing partons.



JHEP07(2017)107

| Objects | Particle- (Parton-) level selection |
|---|---|
| Leptons | $p_{\mathrm{T}}^{\ell} > 25\,\mathrm{GeV}$ and $\lvert\eta^{\ell}\rvert < 2.5$<br>Dressed leptons, OS charge |
| Photon (kinematics) | $E_{\mathrm{T}}^{\gamma} > 15\,\mathrm{GeV}$, $\lvert\eta^{\gamma}\rvert < 2.37$<br>$\Delta R(\ell,\gamma) > 0.4$ |
| Photon (isolation) | $E_{\mathrm{T}}^{\mathrm{iso}} < 0.5 \cdot E_{\mathrm{T}}^{\gamma}$ (no isolation) |
| FSR cut | $m_{\ell\ell} + m_{\ell\ell\gamma} > 182\,\mathrm{GeV}$<br>$m_{\ell\ell} > 40$ GeV |
| Particle jets (Outgoing partons)<br>($j$ = jets)<br>($p$ = outgoing quarks or gluons) | At least two jets (outgoing partons)<br>$E_{\mathrm{T}}^{j(p)} > 30$ GeV, $\lvert\eta^{j(p)}\rvert < 4.5$<br>$\Delta R(\ell, j(p)) > 0.3$<br>$\Delta R(\gamma, j(p)) > 0.4$ |
| Control region (CR) | $150 < m_{jj(pp)} < 500$ GeV |
| Search region (SR) | $m_{jj(pp)} > 500$ GeV |
| aQGC region | $m_{jj(pp)} > 500$ GeV<br>$E_{\mathrm{T}}^{\gamma} > 250$ GeV |

**Table 5**. Charged-lepton channel phase-space region definitions at particle level (parton level when different) for both $pp \to Z\gamma jj$ EWK and QCD production. If there are more than two jets/final-state partons, the two highest transverse momentum ones are considered.

In order to compare the measured fiducial cross-section (at particle level) with the NLO theory predictions by VBFNLO (at parton level) [48], a correction factor $A^{\mathrm{parton}}$ is derived. Such a correction accounts for differences between the parton- and particle-level phase-space regions. It is defined as the ratio of the number of generated events in the parton-level phase-space region to the number of events in the particle-level phase-space region, and it depends on fragmentation and hadronization models implemented in MC event generators. Using the $Z\gamma jj$ EWK SHERPA MC simulation, $A^{\mathrm{parton}}$ is found to be 1.02 and 0.86 for the CR and SR respectively (with negligible statistical uncertainty).

### 6.1 Fiducial electroweak production cross-section determination

The determination of the fiducial cross-section is carried out using the signal strength parameter $\mu$

$$\mu = \frac{N_{\mathrm{data}}^{\mathrm{signal}}}{N_{\mathrm{MC}}^{\mathrm{signal}}} = \frac{\sigma_{\mathrm{data}}}{\sigma_{\mathrm{MC}}}, \tag{6.1}$$

where $N_{\mathrm{data}}^{\mathrm{signal}}$ is the signal yield in the data and $N_{\mathrm{MC}}^{\mathrm{signal}}$ is the number of signal events predicted by the SHERPA MC simulation, with selection efficiencies extracted from data. The measured cross-section $\sigma_{\mathrm{data}}$ is derived from the signal strength by multiplying it by the SHERPA MC cross-section prediction $\sigma_{\mathrm{MC}}$ in the fiducial region.

The signal strength is extracted using a likelihood fit over the centrality of the $Z\gamma$ two-body system, $\zeta_{Z\gamma}$ (see equation (4.1) and figure 5), which provides good discrimination between the EWK and QCD production processes. Probability density functions are built [49] from binned histograms of $\zeta_{Z\gamma}$ distributions (referred to as templates) using MC



JHEP07(2017)107

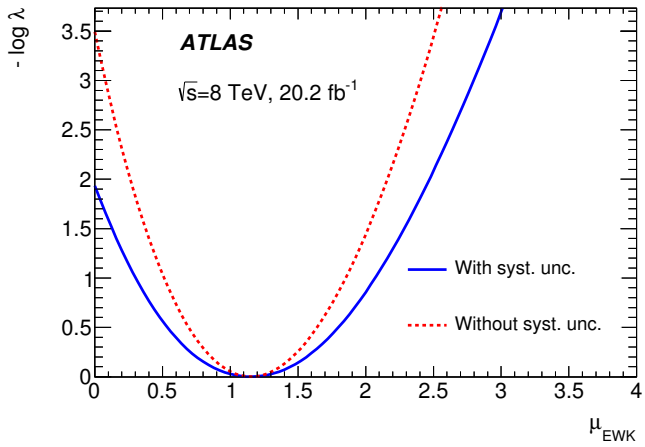


**Figure 7**. The profile of the negative log-likelihood ratio $\lambda(\mu_{\mathrm{EWK}})$ of the signal strength $\mu_{\mathrm{EWK}}$ of the $\zeta_{Z\gamma}$ template. The observed result is shown by the solid curve, while the dashed curve shows the results with only the statistical uncertainty included. The observed significance of the measurement is given by $\sqrt{-2\log\lambda(0)}$ and equals $2.0\sigma$ in this case.

events for signal and each of the backgrounds described in section 5. The interference between the EWK and QCD induced processes is not included in the probability density functions but rather taken as an uncertainty ($\sim 7\%$ of the signal yield, determined with Sherpa MC samples).

An extended likelihood is built from the product of four likelihoods corresponding to $\zeta_{Z\gamma}$ distributions in the SR and CR for the electron channel and the SR and CR for the muon channel. The inclusion of the CR likelihoods in the fit (where the EWK signal process is suppressed) provides a strong constraint on the QCD process normalization in the SR. The QCD normalization is introduced in the likelihood as a single parameter for both the CR and the SR. It is treated as an unconstrained nuisance parameter and mainly determined by the data in the CR, where events from the QCD process dominate. The normalizations and shapes of the other backgrounds are taken from MC predictions and can vary within the uncertainties reported in section 5.

The signal strength for the EWK production, $\mu_{\mathrm{EWK}}$, and its uncertainty are determined with a profile-likelihood-ratio test statistic [50]. Systematic uncertainties in the input templates are handled using nuisance parameters corresponding to each systematic effect, which are assumed to have Gaussian distributions with standard deviation $\sigma$ equal to the systematic uncertainty in the parameter in question. The profile of the negative log-likelihood ratio of the signal strength $\mu_{\mathrm{EWK}}$ is shown in figure 7.

From the best-fit value of $\mu_{\mathrm{EWK}}$, the observed $Z\gamma jj$ EWK production fiducial cross-section in the SR defined in table 5, is found to be:

$$\sigma^{\mathrm{EWK}}_{Z\gamma jj} = 1.1 \pm 0.5\ (\mathrm{stat}) \pm 0.4\ (\mathrm{syst})\ \mathrm{fb} = 1.1 \pm 0.6\ \mathrm{fb}.$$

while the SM NLO prediction [48] from Vbfnlo, after applying the $A^{\mathrm{parton}}$ correction



JHEP07(2017)107

| Source of uncertainty | EWK [%] | Total (EWK+QCD) [%] SR | CR |
|---|---|---|---|
| Statistical | 40 | 9 | 4 |
| Jet energy scale | 36 | 9 | 4 |
| Theory | 10 | 5 | 4 |
| All other | 8 | 5 | 6 |
| Total systematic | 38 | 11 | 8 |

**Table 6**. Summary of the main relative uncertainties in cross-section measurements presented in this paper.

described above, and with uncertainties calculated as described in section 3, is

$$\sigma_{Z\gamma jj}^{\text{VBFNLO,EWK}} = 0.94 \pm 0.09\,\text{fb}.$$

The significance of the observed EWK production signal is $2.0\sigma$ ($1.8\sigma$ expected), not large enough to claim an observation of this process. The measured 95% confidence level (CL) cross-section upper limit obtained with the $CL_S$ technique [50] is 2.2 fb. A breakdown of the uncertainties of the $\sigma_{Z\gamma jj}^{\text{EWK}}$ cross-section measurement, as well as the total (EWK+QCD) cross-sections discussed in the next section, is given in table 6.

The statistical uncertainty of the measurement of $\sigma_{Z\gamma jj}^{\text{EWK}}$ is 40%. The 38% systematic uncertainty is dominated by the 36% jet energy scale (JES) uncertainty contribution. In particular, the contribution of the uncertainty in the $\eta$-intercalibration method of the JES is quite large, since events at low $\zeta_{Z\gamma}$ tend to have jets with high rapidity. This uncertainty strongly affects both the normalization and the shape of the EWK and QCD $\zeta_{Z\gamma}$ distribution. The impact of the JES uncertainty in the shape of the $\zeta_{Z\gamma}$ distributions increases the normalization-only uncertainty by about 40%, and affects the SR and CR uncertainties by different amounts. As a consequence, the constraint from CR data is not as effective in reducing the JES uncertainty as it is for other systematic uncertainties. Nonetheless, the use of the CR data reduces the total systematic uncertainty of the EWK cross-section measurement in the SR from about 60% to 38%.

The second largest contribution to the systematic uncertainty is from the theory uncertainty (Sherpa modelling of the $Z\gamma jj$ production processes and interference between the QCD and EWK processes) and amounts to 10%, while all other contributions combined (photon and lepton identification, reconstruction, isolation and energy scale, and uncertainty from the $Z$+jet background estimate) are around 8%.

The post-fit QCD production normalization is found to be in agreement with the Sherpa predictions within one standard deviation. Cross-sections extracted separately in the electron and muon channels are also compatible within their statistical uncertainty.

### 6.2 Total $Z\gamma jj$ fiducial cross-section measurements

The total $Z\gamma jj$ production (QCD+EWK) cross-section in the SR and CR is extracted from data with a slight modification of the template fit method described in section 6.1. In this case both the EWK and QCD $Z\gamma jj$ production are considered as signal. As a consequence



JHEP07(2017)107

| Channel | Phase-space region | Process type | Measured cross-section [fb] | Predicted cross-section [fb] |
|---|---|---|---|---|
| $Z(\ell^+\ell^-)\gamma jj$ | Search region | EWK | $1.1 \pm 0.5$ (stat) $\pm 0.4$ (syst) | $0.94 \pm 0.09$ |
| $Z(\ell^+\ell^-)\gamma jj$ | Search region | EWK+QCD | $3.4 \pm 0.3$ (stat) $\pm 0.4$ (syst) | $4.0 \pm 0.4$ |
| $Z(\ell^+\ell^-)\gamma jj$ | Control region | EWK+QCD | $21.9 \pm 0.9$ (stat) $\pm 1.8$ (syst) | $22.9 \pm 1.9$ |

**Table 7**. Summary of $Z\gamma jj$ production cross-section measurements in the search and control regions for the charged-lepton channel.

a unique signal strength $\mu_{Z\gamma jj}$ for the total QCD and EWK production is used, and hence the relative ratio of QCD and EWK contributions is fixed to the Sherpa MC predicted value. The SR and CR phase-space regions are treated independently and $\mu_{Z\gamma jj}$ is not assumed to be the same in the two regions. As before, $\zeta_{Z\gamma}$ templates are taken from the separate Sherpa MC samples of the EWK and QCD production.

EWK-QCD interference is negligible with respect to the total production and is not considered.

From the best-fit value of $\mu_{Z\gamma jj}$, the measured total $Z\gamma jj$ production cross-section in the SR and CR is found to be:

$$\sigma^{\mathrm{SR}}_{Z\gamma jj} = 3.4 \pm 0.3\ (\mathrm{stat}) \pm 0.4\ (\mathrm{syst})\ \mathrm{fb} = 3.4 \pm 0.5\ \mathrm{fb},$$
$$\sigma^{\mathrm{CR}}_{Z\gamma jj} = 21.9 \pm 0.9\ (\mathrm{stat}) \pm 1.8\ (\mathrm{syst})\ \mathrm{fb} = 21.9 \pm 2.0\ \mathrm{fb}.$$

The cross-sections measured separately in the electron and muon channels are compatible within their statistical uncertainty.

In both measurements, the systematic uncertainty (11% and 8% in the SR and CR respectively) dominates over the statistical uncertainty (9% and 4% in the SR and CR respectively). A summary of the main sources of systematic uncertainty is given in table 6.

The total $Z\gamma jj$ cross-section predictions at QCD NLO [48] are derived adding the individual Vbfnlo QCD and EWK production predictions with uncertainties calculated as described in section 3. They are found to be:

$$\sigma^{\mathrm{VBFNLO,SR}}_{Z\gamma jj} = 4.0 \pm 0.4\ \mathrm{fb},$$
$$\sigma^{\mathrm{VBFNLO,CR}}_{Z\gamma jj} = 22.9 \pm 1.9\ \mathrm{fb}.$$

These predictions include $A^{\mathrm{parton}}$ corrections derived from Sherpa MC samples reported before for EWK production as well as $A^{\mathrm{parton}}$ corrections for QCD production, which are 0.76 and 0.82 in the CR and SR respectively, with negligible statistical uncertainty.

A summary of the $Z\gamma jj$ production cross-section measurements in the charged-lepton channel is given in table 7. In both the SR and CR, and for both electroweak $Z\gamma jj$ and total $Z\gamma jj$ production, the Vbfnlo MC predictions describe the data well.

## 7 Limits on quartic gauge-boson couplings

Since QGCs contribute to VBS processes in the SM, the $Z\gamma jj$ EWK production, which contains VBS processes, can be used to probe new physics via anomalies in the extracted



JHEP07(2017)107

coupling values. $Z\gamma jj$ EWK production in the SM has no contributions at the tree level from the neutral QGCs of $ZZZ\gamma$, $ZZ\gamma\gamma$ and $Z\gamma\gamma\gamma$ which consist of only the vector bosons with zero electric charges, but does contain the charged QGC $WWZ\gamma$ vertex with the presence of charged vector bosons in the couplings. New physics beyond the SM could induce charged and neutral anomalous QGCs, enhancing the $Z\gamma jj$ electroweak production cross-section and modifying the kinematic distributions of the final-state bosons.

In this section, events selected in the neutrino channel and in the "aQGC region" for the charged-lepton channel are used to probe aQGC contributions to the $Z\gamma jj$ EWK production, whose relative size is expected to increase with the photon transverse energy. Optimization studies performed on MC samples show that the selection of events with $E_{\mathrm{T}}^{\gamma} > 250\,\mathrm{GeV}$ ($E_{\mathrm{T}}^{\gamma} > 150\,\mathrm{GeV}$) for the charged-lepton (neutrino) channel maximizes the sensitivity to aQGC contributions for the available amount of data. Figures 8 and 9 show the photon transverse energy distribution in the charged-lepton and neutrino channel, respectively, for the data as well as the expected signal and backgrounds, along with one possible aQGC contribution.

### 7.1 Fiducial EWK production cross-section limits in high-$E_{\mathrm{T}}^{\gamma}$ regions

In this section, limits on the fiducial cross-section of $Z\gamma jj$ EWK production in the charged-lepton and neutrino channels in the high-$E_{\mathrm{T}}^{\gamma}$ energy region dedicated to aQGC studies are reported. The fiducial phase-space region definition for the neutrino (charged-lepton) channel is provided in table 8 (table 5). These selections follow closely the experimental selection reported in section 4.3, with MC particle-level objects defined as in section 6.

For both channels, cross-sections are extracted from data using a log-likelihood fit method, where the likelihood function is constructed from a Poisson distribution for the expected number of signal and background events in the aQGC region and Gaussian constraints for nuisance parameters associated with systematic uncertainties. These systematic uncertainties are summarized in table 4.

The $Z\gamma jj$ EWK cross-sections predicted by the SM in these high-$E_{\mathrm{T}}^{\gamma}$ fiducial regions are very small: $(71 \pm 7)$ ab and $(17 \pm 2)$ ab for the neutrino and charged-lepton channels, respectively. Therefore, with $20.2\,\mathrm{fb}^{-1}$ of data only cross-section upper limits are extracted.

Using the Sherpa MC simulation, reconstruction efficiencies, defined as the number of reconstructed MC events passing the event selection divided by the number of generated events at particle level within the fiducial region, are found to be $C_{\mathrm{EWK}}^{\nu\bar{\nu}\gamma jj} = 0.54 \pm 0.03$ and $C_{\mathrm{EWK}}^{\ell^+\ell^-\gamma jj} = 0.56 \pm 0.03$. These factors account for photon and lepton reconstruction, identification, isolation, trigger and jet identification efficiencies and related systematic uncertainties.

The numbers of observed events for the neutrino and charged-lepton channels are four and two, respectively. The 95% CL cross-section upper limits obtained with the $CL_S$ technique are 1.06 fb (0.99 fb expected) in the neutrino channel and 1.03 fb (1.01 fb expected) in the charged-lepton channel.



JHEP07(2017)107

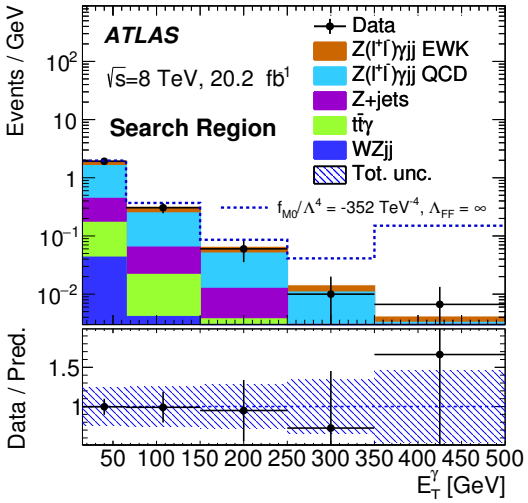


**Figure 8**. Distributions of the photon transverse energy for the electron and muon channels added together in the search region, for the data (black points), and for the signal process and various background components (coloured templates) before any fit is done. The sum of the signal prediction with one non-zero aQGC parameter and the various backgrounds discussed in the text is also shown (blue dashed line). The ratio between data and the sum of all pre-fit expected contributions ("Pred.") is shown below the histogram. The hatched blue band shows the systematic and statistical uncertainty added in quadrature ("Tot. unc.") in the signal and background prediction, while the error bars on the data points represent the statistical uncertainty of the data set. The number of events in each bin is divided by the bin width. The last bin also includes events beyond the range shown.

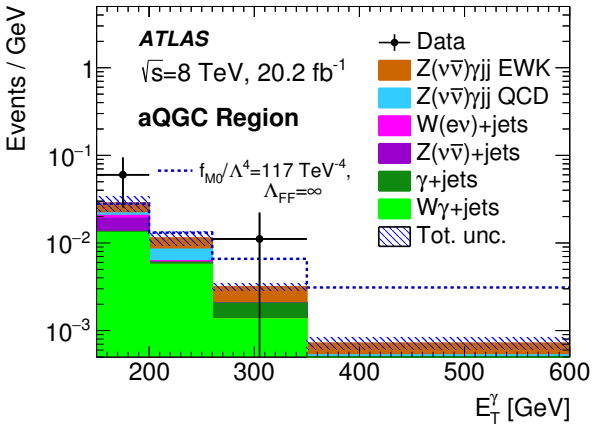


**Figure 9**. Distributions of the photon transverse energy for the neutrino channel in the aQGC region, for the data (black points), and for the signal process and various background components (coloured templates). The sum of the signal prediction with one non-zero aQGC parameter and the various backgrounds discussed in the text is also shown (blue dashed line). The hatched blue band shows the systematic and statistical uncertainty added in quadrature ("Tot. unc.") in the signal and background prediction, while the error bars on the data points represent the statistical uncertainty of the data set. The number of events in each bin is divided by the bin width. The last bin also includes events beyond the range shown.



JHEP07(2017)107

| Objects | Particle- (Parton-) level selection |
|---|---|
| Neutrinos | $E_{\mathrm{T}}^{\nu\bar{\nu}} > 100\,\mathrm{GeV}$ |
| Photon (kinematics) | $E_{\mathrm{T}}^{\gamma} > 150\,\mathrm{GeV}$, $\lvert\eta^{\gamma}\rvert < 2.37$<br>$\Delta R(\ell,\gamma) > 0.4$ |
| Photon (isolation) | $E_{\mathrm{T}}^{\mathrm{iso}} < 0.5 \cdot E_{\mathrm{T}}^{\gamma}$ |
| Generator-level jets (Outgoing quarks)<br>($pp \to Z\gamma qq$) | At least two jets (quarks)<br>$E_{\mathrm{T}}^{j(q)} > 30$ GeV, $\lvert\eta^{j(q)}\rvert < 4.5$<br>$\Delta R(\gamma, j(q)) > 0.4$ |
| Event kinematic selection | $\lvert\Delta\phi(E_{\mathrm{T}}^{\nu\bar{\nu}}, \gamma jj(qq))\rvert > \frac{3\pi}{4}$<br>$\lvert\Delta\phi(E_{\mathrm{T}}^{\nu\bar{\nu}}, \gamma)\rvert > \frac{\pi}{2}$<br>$\lvert\Delta\phi(E_{\mathrm{T}}^{\nu\bar{\nu}}, j(q))\rvert > 1$<br>$E_{\mathrm{T}}^{\gamma} > 150$ GeV<br>$\lvert\Delta y_{jj(qq)}\rvert > 2.5$<br>$\zeta_{\gamma} < 0.3$<br>$p_{\mathrm{T}}^{\mathrm{balance}} < 0.1$<br>$m_{jj(qq)} > 600$ GeV |

**Table 8**. Neutrino channel aQGC region definition at particle (parton) level. If there are more than two jets at particle level, the two highest transverse momentum ones are considered.

### 7.2 Extracting confidence intervals on anomalous quartic gauge-boson couplings.

An effective field theory (EFT) [4] with higher-dimensional operators [2] is adopted to parameterize the anomalous couplings. These operators are in the linear Higgs-doublet representation [2, 3].

A parity-conserving EFT Lagrangian is constructed based on the hypothesis that the observed Higgs boson belongs to an $\mathrm{SU}(2)_{\mathrm{L}}$ doublet [2] and has the form

$$\mathcal{L} = \mathcal{L}^{\mathrm{SM}} + \sum_{i} \frac{c_i}{\Lambda^2}\mathcal{O}_i + \sum_{j} \frac{f_j}{\Lambda^4}\mathcal{O}_j. \tag{7.1}$$

The first term represents the SM lagrangian, while higher-order terms represent new physics inducing anomalous gauge couplings, such as the dimension-6 term (second term) and dimension-8 term (third term) with all components of each term summed up according to the dimension of the new physics scale $\Lambda$ [3, 4]. Out of these higher-order operators, the dimension-8 ones are the lowest-dimension operators inducing only quartic gauge-boson couplings without triple gauge-boson vertices. The dimension-8 operators with coefficients $f_j$ are sub-categorized in $f_{T,x}$ operators, containing only the field-strength tensor, and $f_{M,x}$ operators, containing both the Higgs $\mathrm{SU}(2)_{\mathrm{L}}$ doublet derivatives and the field strength. The charged anomalous couplings of $WWZ\gamma$ can be induced only by the $f_{M,x}$ ($x$=0–7) and $f_{T,x}$ ($x$=0–7) operators. The neutral aQGCs of $ZZZ\gamma$ and $ZZ\gamma\gamma$ can be induced by



JHEP07(2017)107

the $f_{M,x}$ ($x$=0–7) and $f_{T,x}$ ($x$=0–9) operators while $Z\gamma\gamma\gamma$ QGC can be modified only by $f_{T,x}$ ($x$=0–9) operators.

Only a subset of these dimension-8 operators are probed here with events from $Z\gamma jj$ EWK production: $f_{T0}/\Lambda^4$, as a representative operator of $f_{T1}/\Lambda^4$ and $f_{T2}/\Lambda^4$; $f_{T8}/\Lambda^4$ and $f_{T9}/\Lambda^4$, the two unique operators which can be probed only via neutral QGC vertices; and $f_{M0}/\Lambda^4$, $f_{M1}/\Lambda^4$, $f_{M2}/\Lambda^4$ and $f_{M3}/\Lambda^4$, which allow comparisons and possible combinations with results from other experiments.

Form factors (FF) must be introduced to restore unitarity at very high parton centre-of-mass energy $\sqrt{\hat{s}}$: $f_i(\hat{s}) = f_i/(1+\hat{s}/\Lambda_{\rm FF}^2)^n$, where $\Lambda_{\rm FF}$ is the parameter chosen to prevent unitarity violation up to $\sqrt{\hat{s}} = 8$ TeV and the FF exponent is set to $n = 2$.

Data in the aQGC regions, defined in tables 5 and 8 for the charged-lepton and neutrino channels respectively, are used. These phase-space regions are determined by optimizing the expected confidence intervals on the dimension-8 operator coefficients in the individual channels.

MC $Z\gamma jj$ EWK events with non-zero EFT dimension-8 operator coefficients are generated by MadGraph 5.1 [23] at LO, interfaced with Pythia 6 [51] for parton showering, and processed through the ATLAS detector full simulation, for both the charged-lepton and the neutrino channels. One MC sample is generated for each of the dimension-8 operators to study the aQGC event selection efficiencies. The difference with respect to the selection efficiency calculated from SM samples modelled with Sherpa is taken as an additional uncertainty of 20%(10%) for the charged-lepton (neutrino) channel analysis. The event yields from background physics processes sensitive to aQGC probed here are kept fixed to SM predictions.

The aQGC cross-sections are calculated at NLO precision in $\alpha_{\rm s}$ [48] using the Vbfnlo event generator and parameterized as a function of the dimension-8 operator anomalous coupling values. For each operator, the cross-sections are calculated for five aQGC coupling values. A parabola is then fit to parameterize the cross-section as a function of the operator coefficient.

For both channels, a one-dimensional profile-likelihood fit is used to derive the expected and observed 95% CL intervals of each dimension-8 operator coefficient, with all the other operator coefficients set to zero. The neutrino channel provides the best expected intervals for all operators. However, they are improved by 10–30% when the results from both channels are combined. The channel combination is obtained taking into account correlations between systematic uncertainties. In particular, the systematic uncertainties of the photon identification efficiency, uncertainties due to the jet energy scale and resolution, PDF uncertainties, uncertainties in parton-shower modelling, and the systematic uncertainty on the QCD renormalisation and factorization scales are considered as correlated. Among these systematic uncertainties, the QCD renormalization and factorization scale uncertainties are the leading ones, and are 8.0% (7.7%) in the charged-lepton (neutrino) channel.

Table 9 shows the expected and observed 95% CL intervals derived with the $\Lambda_{\rm FF}$ set to the maximum allowed value to preserve unitarity, according to the Vbfnlo calculation. The expected and observed 95% CL intervals derived without respecting the unitarity bounds ($n = 0$) and without other unitarization restrictions are also reported in table 9.



JHEP07(2017)107

| | 95% CL intervals | Measured [TeV$^{-4}$] | Expected [TeV$^{-4}$] | $\Lambda_{\mathrm{FF}}$ [TeV] |
|---|---|---|---|---|
| $n = 0$ | $f_{T9}/\Lambda^4$ | $[-4.1, 4.2] \times 10^3$ | $[-2.9, 3.0] \times 10^3$ | |
| | $f_{T8}/\Lambda^4$ | $[-1.9, 2.1] \times 10^3$ | $[-1.2, 1.7] \times 10^3$ | |
| | $f_{T0}/\Lambda^4$ | $[-1.9, 1.6] \times 10^1$ | $[-1.6, 1.3] \times 10^1$ | |
| | $f_{M0}/\Lambda^4$ | $[-1.6, 1.8] \times 10^2$ | $[-1.4, 1.5] \times 10^2$ | |
| | $f_{M1}/\Lambda^4$ | $[-3.5, 3.4] \times 10^2$ | $[-3.0, 2.9] \times 10^2$ | |
| | $f_{M2}/\Lambda^4$ | $[-8.9, 8.9] \times 10^2$ | $[-7.5, 7.5] \times 10^2$ | |
| | $f_{M3}/\Lambda^4$ | $[-1.7, 1.7] \times 10^3$ | $[-1.4, 1.4] \times 10^3$ | |
| $n = 2$ | $f_{T9}/\Lambda^4$ | $[-6.9, 6.9] \times 10^4$ | $[-5.4, 5.3] \times 10^4$ | 0.7 |
| | $f_{T8}/\Lambda^4$ | $[-3.4, 3.3] \times 10^4$ | $[-2.6, 2.5] \times 10^4$ | 0.7 |
| | $f_{T0}/\Lambda^4$ | $[-7.2, 6.1] \times 10^1$ | $[-6.1, 5.0] \times 10^1$ | 1.7 |
| | $f_{M0}/\Lambda^4$ | $[-1.0, 1.0] \times 10^3$ | $[-8.8, 8.8] \times 10^2$ | 1.0 |
| | $f_{M1}/\Lambda^4$ | $[-1.6, 1.7] \times 10^3$ | $[-1.4, 1.4] \times 10^3$ | 1.2 |
| | $f_{M2}/\Lambda^4$ | $[-1.1, 1.1] \times 10^4$ | $[-9.2, 9.6] \times 10^3$ | 0.7 |
| | $f_{M3}/\Lambda^4$ | $[-1.6, 1.6] \times 10^4$ | $[-1.4, 1.3] \times 10^4$ | 0.8 |

**Table 9**. Measured and expected one-dimensional 95% confidence level intervals on aQGC parameters (in the VBFNLO formalism) using the combination of all $Z\gamma jj$ channels (charged-lepton and neutrino). The FF exponent $n = 0$ entries correspond to an infinite FF scale and therefore result in non-unitarized 95% CL intervals. FF exponent $n = 2$ confidence intervals preserve unitarity with individual form-factor scales as shown in the last column for each dimension-8 operator. The maximum allowed form-factor values $\Lambda_{\mathrm{FF}}$ are chosen, according to the unitarity bounds calculated by VBFNLO and are also reported in this table. The latest NLO cross-section prediction of VBFNLO is used in the aQGC parameterization [48].

## 8 Conclusions

Studies of electroweak production of a $Z$ boson and a photon in association with a high-mass dijet system, with the $Z$ boson decaying into a pair of either electrons, muons, or neutrinos, have been performed using 20.2 fb$^{-1}$ of proton-proton collision data at $\sqrt{s} = 8$ TeV collected by the ATLAS experiment at the LHC.

In the charged-lepton channel, the $Z\gamma jj$ EWK production cross-section in a fiducial region with a signal purity of about 18% is found to be:

$$\sigma^{\mathrm{EWK}}_{Z\gamma jj} = 1.1 \pm 0.6\,\mathrm{fb},$$

which is consistent with the NLO SM prediction from VBFNLO, and corresponds to a significance of $2\sigma$. The total $Z\gamma jj$ production cross-section is also measured in the same fiducial region and in a phase-space region dominated by QCD production and both are found to be in good agreement with the NLO SM predictions from VBFNLO.

Events with high-$E_{\mathrm{T}}$ photons in both the charged-lepton and neutrino decay modes of the $Z$ boson are used to extract confidence intervals on seven different aQGC parameters



JHEP07(2017)107

modelled by dimension-8 operators of an effective field theory. In both channels, 95% CL upper limits on the SM $Z\gamma jj$ EWK production cross-sections are placed in these high-$E_{\mathrm{T}}$ photon phase-space regions. The 95% CL intervals on the aQGC parameters are competitive or even more stringent than previous constraints obtained with events with $Z\gamma jj$ and different final states.

## Acknowledgments

We thank CERN for the very successful operation of the LHC, as well as the support staff from our institutions without whom ATLAS could not be operated efficiently.

We acknowledge the support of ANPCyT, Argentina; YerPhI, Armenia; ARC, Australia; BMWFW and FWF, Austria; ANAS, Azerbaijan; SSTC, Belarus; CNPq and FAPESP, Brazil; NSERC, NRC and CFI, Canada; CERN; CONICYT, Chile; CAS, MOST and NSFC, China; COLCIENCIAS, Colombia; MSMT CR, MPO CR and VSC CR, Czech Republic; DNRF and DNSRC, Denmark; IN2P3-CNRS, CEA-DSM/IRFU, France; SRNSF, Georgia; BMBF, HGF, and MPG, Germany; GSRT, Greece; RGC, Hong Kong SAR, China; ISF, I-CORE and Benoziyo Center, Israel; INFN, Italy; MEXT and JSPS, Japan; CNRST, Morocco; NWO, Netherlands; RCN, Norway; MNiSW and NCN, Poland; FCT, Portugal; MNE/IFA, Romania; MES of Russia and NRC KI, Russian Federation; JINR; MESTD, Serbia; MSSR, Slovakia; ARRS and MIZŠ, Slovenia; DST/NRF, South Africa; MINECO, Spain; SRC and Wallenberg Foundation, Sweden; SERI, SNSF and Cantons of Bern and Geneva, Switzerland; MOST, Taiwan; TAEK, Turkey; STFC, United Kingdom; DOE and NSF, United States of America. In addition, individual groups and members have received support from BCKDF, the Canada Council, CANARIE, CRC, Compute Canada, FQRNT, and the Ontario Innovation Trust, Canada; EPLANET, ERC, ERDF, FP7, Horizon 2020 and Marie Skłodowska-Curie Actions, European Union; Investissements d'Avenir Labex and Idex, ANR, Région Auvergne and Fondation Partager le Savoir, France; DFG and AvH Foundation, Germany; Herakleitos, Thales and Aristeia programmes co-financed by EU-ESF and the Greek NSRF; BSF, GIF and Minerva, Israel; BRF, Norway; CERCA Programme Generalitat de Catalunya, Generalitat Valenciana, Spain; the Royal Society and Leverhulme Trust, United Kingdom.

The crucial computing support from all WLCG partners is acknowledged gratefully, in particular from CERN, the ATLAS Tier-1 facilities at TRIUMF (Canada), NDGF (Denmark, Norway, Sweden), CC-IN2P3 (France), KIT/GridKA (Germany), INFN-CNAF (Italy), NL-T1 (Netherlands), PIC (Spain), ASGC (Taiwan), RAL (UK) and BNL (USA), the Tier-2 facilities worldwide and large non-WLCG resource providers. Major contributors of computing resources are listed in ref. [52].





JHEP07(2017)107

## References


[1] O.J.P. Eboli, M.C. Gonzalez-Garcia and S.M. Lietti, *Bosonic quartic couplings at CERN LHC*, *Phys. Rev.* **D 69** (2004) 095005 [hep-ph/0310141] [INSPIRE].

[2] O.J.P. Eboli, M.C. Gonzalez-Garcia and J.K. Mizukoshi, $pp \to jje^{\pm}\mu^{\pm}\nu\nu$ *and* $jje^{\pm}\mu^{\mp}\nu\nu$ *at* $O(\alpha_{em}^6)$ *and* $O(\alpha_{em}^4\alpha_s^2)$ *for the study of the quartic electroweak gauge boson vertex at CERN LHC*, *Phys. Rev.* **D 74** (2006) 073005 [hep-ph/0606118] [INSPIRE].

[3] M. Baak et al., *Study of Electroweak Interactions at the Energy Frontier*, arXiv:1310.6708 [INSPIRE].

[4] C. Degrande et al., *Effective field theory: a modern approach to anomalous couplings*, *Annals Phys.* **335** (2013) 21 [arXiv:1205.4231] [INSPIRE].

[5] C. Arzt, M.B. Einhorn and J. Wudka, *Patterns of deviation from the standard model*, *Nucl. Phys.* **B 433** (1995) 41 [hep-ph/9405214] [INSPIRE].

[6] CMS collaboration, *Search for* $WW\gamma$ *and* $WZ\gamma$ *production and constraints on anomalous quartic gauge couplings in pp collisions at* $\sqrt{s} = 8$ *TeV*, *Phys. Rev.* **D 90** (2014) 032008 [arXiv:1404.4619] [INSPIRE].

[7] ATLAS collaboration, *Evidence of* $W\gamma\gamma$ *Production in pp Collisions at* $\sqrt{s} = 8$ *TeV and Limits on Anomalous Quartic Gauge Couplings with the ATLAS Detector*, *Phys. Rev. Lett.* **115** (2015) 031802 [arXiv:1503.03243] [INSPIRE].

[8] CMS collaboration, *Measurements of the* $pp \to W\gamma\gamma$ *and* $pp \to Z\gamma\gamma$ *cross sections and limits on anomalous quartic gauge couplings at* $\sqrt{s} = 8$ *TeV*, arXiv:1704.00366 [INSPIRE].

[9] ATLAS collaboration, *Measurements of* $Z\gamma$ *and* $Z\gamma\gamma$ *production in pp collisions at* $\sqrt{s} = 8$ *TeV with the ATLAS detector*, *Phys. Rev.* **D 93** (2016) 112002 [arXiv:1604.05232] [INSPIRE].

[10] ATLAS collaboration, , *Search for triboson* $W^{\pm}W^{\pm}W^{\mp}$ *production in pp collisions at* $\sqrt{s} = 8$ *TeV with the ATLAS detector*, *Eur. Phys. J.* **C 77** (2017) 141 [arXiv:1610.05088] [INSPIRE].

[11] CMS collaboration, *Study of exclusive two-photon production of* $W^+W^-$ *in pp collisions at* $\sqrt{s} = 7$ *TeV and constraints on anomalous quartic gauge couplings*, *JHEP* **07** (2013) 116 [arXiv:1305.5596] [INSPIRE].

[12] ATLAS collaboration, *Measurement of exclusive* $\gamma\gamma \to W^+W^-$ *production and search for exclusive Higgs boson production in pp collisions at* $\sqrt{s} = 8$ *TeV using the ATLAS detector*, *Phys. Rev.* **D 94** (2016) 032011 [arXiv:1607.03745] [INSPIRE].

[13] ATLAS collaboration, *Measurement of* $W^{\pm}W^{\pm}$ *vector-boson scattering and limits on anomalous quartic gauge couplings with the ATLAS detector*, arXiv:1611.02428 [INSPIRE].

[14] ATLAS collaboration, *Search for anomalous electroweak production of* $WW/WZ$ *in association with a high-mass dijet system in pp collisions at* $\sqrt{s} = 8$ *TeV with the ATLAS detector*, *Phys. Rev.* **D 95** (2017) 032001 [arXiv:1609.05122] [INSPIRE].

[15] CMS collaboration, *Measurement of the cross section for electroweak production of* $Z\gamma$ *in association with two jets and constraints on anomalous quartic gauge couplings in proton–proton collisions at* $\sqrt{s} = 8$ *TeV*, *Phys. Lett.* **B 770** (2017) 380 [arXiv:1702.03025] [INSPIRE].

[16] CMS collaboration, *Measurement of electroweak-induced production of* $W\gamma$ *with two jets in pp collisions at* $\sqrt{s} = 8$ *TeV and constraints on anomalous quartic gauge couplings*, *JHEP* **06** (2017) 106 [arXiv:1612.09256] [INSPIRE].




JHEP07(2017)107

[17] J.D. Bjorken, *Rapidity gaps and jets as a new physics signature in very high-energy hadron hadron collisions*, *Phys. Rev.* **D 47** (1993) 101 [INSPIRE].

[18] ATLAS collaboration, *The ATLAS Experiment at the CERN Large Hadron Collider*, 2008 *JINST* **3** S08003 [INSPIRE].

[19] ATLAS collaboration, *Luminosity determination in pp collisions at $\sqrt{s} = 8$ TeV using the ATLAS detector at the LHC*, *Eur. Phys. J.* **C 76** (2016) 653 [arXiv:1608.03953] [INSPIRE].

[20] ATLAS collaboration, *The ATLAS Simulation Infrastructure*, *Eur. Phys. J.* **C 70** (2010) 823 [arXiv:1005.4568] [INSPIRE].

[21] GEANT4 collaboration, S. Agostinelli et al., *GEANT4: A Simulation toolkit*, *Nucl. Instrum. Meth.* **A 506** (2003) 250 [INSPIRE].

[22] T. Gleisberg et al., *Event generation with SHERPA 1.1*, *JHEP* **02** (2009) 007 [arXiv:0811.4622] [INSPIRE].

[23] J. Alwall et al., *The automated computation of tree-level and next-to-leading order differential cross sections and their matching to parton shower simulations*, *JHEP* **07** (2014) 079 [arXiv:1405.0301] [INSPIRE].

[24] S. Catani, F. Krauss, R. Kuhn and B.R. Webber, *QCD matrix elements + parton showers*, *JHEP* **11** (2001) 063 [hep-ph/0109231] [INSPIRE].

[25] F. Krauss, *Matrix elements and parton showers in hadronic interactions*, *JHEP* **08** (2002) 015 [hep-ph/0205283] [INSPIRE].

[26] H.-L. Lai et al., *New parton distributions for collider physics*, *Phys. Rev.* **D 82** (2010) 074024 [arXiv:1007.2241] [INSPIRE].

[27] S. Frixione and B.R. Webber, *Matching NLO QCD computations and parton shower simulations*, *JHEP* **06** (2002) 029 [hep-ph/0204244] [INSPIRE].

[28] S. Frixione, F. Stoeckli, P. Torrielli and B.R. Webber, *NLO QCD corrections in HERWIG++ with MC@NLO*, *JHEP* **01** (2011) 053 [arXiv:1010.0568] [INSPIRE].

[29] J.M. Butterworth, J.R. Forshaw and M.H. Seymour, *Multiparton interactions in photoproduction at HERA*, *Z. Phys.* **C 72** (1996) 637 [hep-ph/9601371] [INSPIRE].

[30] J. Pumplin, D.R. Stump, J. Huston, H.L. Lai, P.M. Nadolsky and W.K. Tung, *New generation of parton distributions with uncertainties from global QCD analysis*, *JHEP* **07** (2002) 012 [hep-ph/0201195] [INSPIRE].

[31] T. Sjöstrand, S. Mrenna and P.Z. Skands, *A Brief Introduction to PYTHIA 8.1*, *Comput. Phys. Commun.* **178** (2008) 852 [arXiv:0710.3820] [INSPIRE].

[32] K. Melnikov, M. Schulze and A. Scharf, *QCD corrections to top quark pair production in association with a photon at hadron colliders*, *Phys. Rev.* **D 83** (2011) 074013 [arXiv:1102.1967] [INSPIRE].

[33] ATLAS collaboration, *Summary of ATLAS PYTHIA 8 tunes*, ATL-PHYS-PUB-2012-003 (2012).

[34] A.D. Martin, W.J. Stirling, R.S. Thorne and G. Watt, *Parton distributions for the LHC*, *Eur. Phys. J.* **C 63** (2009) 189 [arXiv:0901.0002] [INSPIRE].

[35] K. Arnold et al., *VBFNLO: A Parton level Monte Carlo for processes with electroweak bosons*, *Comput. Phys. Commun.* **180** (2009) 1661 [arXiv:0811.4559] [INSPIRE].

[36] K. Arnold et al., *VBFNLO: A parton level monte carlo for processes with electroweak bosons — Manual for version 2.7.0*, arXiv:1107.4038 [INSPIRE].

JHEP07(2017)107

[37] K. Arnold et al., *Release Note – Vbfnlo-2.6.0*, arXiv:1207.4975 [INSPIRE].

[38] ATLAS collaboration, *Electron efficiency measurements with the ATLAS detector using 2012 LHC proton–proton collision data*, *Eur. Phys. J.* **C 77** (2017) 195 [arXiv:1612.01456] [INSPIRE].

[39] ATLAS collaboration, *Electron performance measurements with the ATLAS detector using the 2010 LHC proton-proton collision data*, *Eur. Phys. J.* **C 72** (2012) 1909 [arXiv:1110.3174] [INSPIRE].

[40] ATLAS collaboration, *Measurement of the muon reconstruction performance of the ATLAS detector using 2011 and 2012 LHC proton–proton collision data*, *Eur. Phys. J.* **C 74** (2014) 3130 [arXiv:1407.3935] [INSPIRE].

[41] ATLAS collaboration, *Measurement of the photon identification efficiencies with the ATLAS detector using LHC Run-1 data*, *Eur. Phys. J.* **C 76** (2016) 666 [arXiv:1606.01813] [INSPIRE].

[42] M. Cacciari, G.P. Salam and S. Sapeta, *On the characterisation of the underlying event*, *JHEP* **04** (2010) 065 [arXiv:0912.4926] [INSPIRE].

[43] ATLAS collaboration, *Measurement of the inclusive isolated prompt photon cross section in pp collisions at $\sqrt{s} = 7$ TeV with the ATLAS detector*, *Phys. Rev.* **D 83** (2011) 052005 [arXiv:1012.4389] [INSPIRE].

[44] M. Cacciari, G.P. Salam and G. Soyez, *The Anti-k(t) jet clustering algorithm*, *JHEP* **04** (2008) 063 [arXiv:0802.1189] [INSPIRE].

[45] ATLAS collaboration, *Jet energy measurement and its systematic uncertainty in proton-proton collisions at $\sqrt{s} = 7$ TeV with the ATLAS detector*, *Eur. Phys. J.* **C 75** (2015) 17 [arXiv:1406.0076] [INSPIRE].

[46] ATLAS collaboration, *Performance of pile-up mitigation techniques for jets in pp collisions at $\sqrt{s} = 8$ TeV using the ATLAS detector*, *Eur. Phys. J.* **C 76** (2016) 581 [arXiv:1510.03823] [INSPIRE].

[47] ATLAS collaboration, *Performance of Missing Transverse Momentum Reconstruction in Proton-Proton Collisions at 7 TeV with ATLAS*, *Eur. Phys. J.* **C 72** (2012) 1844 [arXiv:1108.5602] [INSPIRE].

[48] F. Campanario, M. Kerner and D. Zeppenfeld, *ZA production in vector-boson scattering at next-to-leading order QCD*, arXiv:1704.01921 [INSPIRE].

[49] (NIKHEF, Amsterdam), *HistFactory: A tool for creating statistical models for use with RooFit and RooStats*, CERN-OPEN-2012-016 (2012).

[50] G. Cowan, K. Cranmer, E. Gross and O. Vitells, *Asymptotic formulae for likelihood-based tests of new physics*, *Eur. Phys. J.* **C 71** (2011) 1554 [*Erratum ibid.* **C 73** (2013) 2501] [arXiv:1007.1727] [INSPIRE].

[51] T. Sjöstrand, S. Mrenna and P.Z. Skands, *PYTHIA 6.4 Physics and Manual*, *JHEP* **05** (2006) 026 [hep-ph/0603175] [INSPIRE].

[52] ATLAS collaboration, *ATLAS Computing Acknowledgements 2016-2017*, ATL-GEN-PUB-2016-002 (2016).

JHEP07(2017)107

## The ATLAS collaboration

M. Aaboud[137d], G. Aad[88], B. Abbott[115], J. Abdallah[8], O. Abdinov[12,*], B. Abeloos[119], S.H. Abidi[161], O.S. AbouZeid[139], N.L. Abraham[151], H. Abramowicz[155], H. Abreu[154], R. Abreu[118], Y. Abulaiti[148a,148b], B.S. Acharya[167a,167b,a], S. Adachi[157], L. Adamczyk[41a], J. Adelman[110], M. Adersberger[102], T. Adye[133], A.A. Affolder[139], T. Agatonovic-Jovin[14], C. Agheorghiesei[28c], J.A. Aguilar-Saavedra[128a,128f], S.P. Ahlen[24], F. Ahmadov[68,b], G. Aielli[135a,135b], S. Akatsuka[71], H. Akerstedt[148a,148b], T.P.A. Åkesson[84], A.V. Akimov[98], G.L. Alberghi[22a,22b], J. Albert[172], M.J. Alconada Verzini[74], M. Aleksa[32], I.N. Aleksandrov[68], C. Alexa[28b], G. Alexander[155], T. Alexopoulos[10], M. Alhroob[115], B. Ali[130], M. Aliev[76a,76b], G. Alimonti[94a], J. Alison[33], S.P. Alkire[38], B.M.M. Allbrooke[151], B.W. Allen[118], P.P. Allport[19], A. Aloisio[106a,106b], A. Alonso[39], F. Alonso[74], C. Alpigiani[140], A.A. Alshehri[56], M. Alstaty[88], B. Alvarez Gonzalez[32], D. Álvarez Piqueras[170], M.G. Alviggi[106a,106b], B.T. Amadio[16], Y. Amaral Coutinho[26a], C. Amelung[25], D. Amidei[92], S.P. Amor Dos Santos[128a,128c], A. Amorim[128a,128b], S. Amoroso[32], G. Amundsen[25], C. Anastopoulos[141], L.S. Ancu[52], N. Andari[19], T. Andeen[11], C.F. Anders[60b], J.K. Anders[77], K.J. Anderson[33], A. Andreazza[94a,94b], V. Andrei[60a], S. Angelidakis[9], I. Angelozzi[109], A. Angerami[38], A.V. Anisenkov[111,c], N. Anjos[13], A. Annovi[126a,126b], C. Antel[60a], M. Antonelli[50], A. Antonov[100,*], D.J. Antrim[166], F. Anulli[134a], M. Aoki[69], L. Aperio Bella[32], G. Arabidze[93], Y. Arai[69], J.P. Araque[128a], V. Araujo Ferraz[26a], A.T.H. Arce[48], R.E. Ardell[80], F.A. Arduh[74], J-F. Arguin[97], S. Argyropoulos[66], M. Arik[20a], A.J. Armbruster[145], L.J. Armitage[79], O. Arnaez[161], H. Arnold[51], M. Arratia[30], O. Arslan[23], A. Artamonov[99], G. Artoni[122], S. Artz[86], S. Asai[157], N. Asbah[45], A. Ashkenazi[155], L. Asquith[151], K. Assamagan[27], R. Astalos[146a], M. Atkinson[169], N.B. Atlay[143], K. Augsten[130], G. Avolio[32], B. Axen[16], M.K. Ayoub[119], G. Azuelos[97,d], A.E. Baas[60a], M.J. Baca[19], H. Bachacou[138], K. Bachas[76a,76b], M. Backes[122], M. Backhaus[32], P. Bagiacchi[134a,134b], P. Bagnaia[134a,134b], H. Bahrasemani[144], J.T. Baines[133], M. Bajic[39], O.K. Baker[179], E.M. Baldin[111,c], P. Balek[175], T. Balestri[150], F. Balli[138], W.K. Balunas[124], E. Banas[42], Sw. Banerjee[176,e], A.A.E. Bannoura[178], L. Barak[32], E.L. Barberio[91], D. Barberis[53a,53b], M. Barbero[88], T. Barillari[103], M-S Barisits[32], T. Barklow[145], N. Barlow[30], S.L. Barnes[36c], B.M. Barnett[133], R.M. Barnett[16], Z. Barnovska-Blenessy[36a], A. Baroncelli[136a], G. Barone[25], A.J. Barr[122], L. Barranco Navarro[170], F. Barreiro[85], J. Barreiro Guimarães da Costa[35a], R. Bartoldus[145], A.E. Barton[75], P. Bartos[146a], A. Basalaev[125], A. Bassalat[119,f], R.L. Bates[56], S.J. Batista[161], J.R. Batley[30], M. Battaglia[139], M. Bauce[134a,134b], F. Bauer[138], H.S. Bawa[145,g], J.B. Beacham[113], M.D. Beattie[75], T. Beau[83], P.H. Beauchemin[165], P. Bechtle[23], H.P. Beck[18,h], K. Becker[122], M. Becker[86], M. Beckingham[173], C. Becot[112], A.J. Beddall[20e], A. Beddall[20b], V.A. Bednyakov[68], M. Bedognetti[109], C.P. Bee[150], T.A. Beermann[32], M. Begalli[26a], M. Begel[27], J.K. Behr[45], A.S. Bell[81], G. Bella[155], L. Bellagamba[22a], A. Bellerive[31], M. Bellomo[154], K. Belotskiy[100], O. Beltramello[32], N.L. Belyaev[100], O. Benary[155,*], D. Benchekroun[137a], M. Bender[102], K. Bendtz[148a,148b], N. Benekos[10], Y. Benhammou[155], E. Benhar Noccioli[179], J. Benitez[66], D.P. Benjamin[48], M. Benoit[52], J.R. Bensinger[25], S. Bentvelsen[109], L. Beresford[122], M. Beretta[50], D. Berge[109], E. Bergeaas Kuutmann[168], N. Berger[5], J. Beringer[16], S. Berlendis[58], N.R. Bernard[89], G. Bernardi[83], C. Bernius[145], F.U. Bernlochner[23], T. Berry[80], P. Berta[131], C. Bertella[35a], G. Bertoli[148a,148b], F. Bertolucci[126a,126b], I.A. Bertram[75], C. Bertsche[45], D. Bertsche[115], G.J. Besjes[39], O. Bessidskaia Bylund[148a,148b], M. Bessner[45], N. Besson[138], C. Betancourt[51], A. Bethani[87], S. Bethke[103], A.J. Bevan[79], R.M. Bianchi[127], O. Biebel[102], D. Biedermann[17], R. Bielski[87], N.V. Biesuz[126a,126b], M. Biglietti[136a], J. Bilbao De Mendizabal[52], T.R.V. Billoud[97], H. Bilokon[50], M. Bindi[57], A. Bingul[20b], C. Bini[134a,134b], S. Biondi[22a,22b], T. Bisanz[57], C. Bittrich[47], D.M. Bjergaard[48], C.W. Black[152], J.E. Black[145], K.M. Black[24],



JHEP07(2017)107

D. Blackburn[140], R.E. Blair[6], T. Blazek[146a], I. Bloch[45], C. Blocker[25], A. Blue[56], W. Blum[86,*], U. Blumenschein[79], S. Blunier[34a], G.J. Bobbink[109], V.S. Bobrovnikov[111,c], S.S. Bocchetta[84], A. Bocci[48], C. Bock[102], M. Boehler[51], D. Boerner[178], D. Bogavac[102], A.G. Bogdanchikov[111], C. Bohm[148a], V. Boisvert[80], P. Bokan[168,i], T. Bold[41a], A.S. Boldyrev[101], A.E. Bolz[60b], M. Bomben[83], M. Bona[79], M. Boonekamp[138], A. Borisov[132], G. Borissov[75], J. Bortfeldt[32], D. Bortoletto[122], V. Bortolotto[62a,62b,62c], D. Boscherini[22a], M. Bosman[13], J.D. Bossio Sola[29], J. Boudreau[127], J. Bouffard[2], E.V. Bouhova-Thacker[75], D. Boumediene[37], C. Bourdarios[119], S.K. Boutle[56], A. Boveia[113], J. Boyd[32], I.R. Boyko[68], J. Bracinik[19], A. Brandt[8], G. Brandt[57], O. Brandt[60a], U. Bratzler[158], B. Brau[89], J.E. Brau[118], W.D. Breaden Madden[56], K. Brendlinger[45], A.J. Brennan[91], L. Brenner[109], R. Brenner[168], S. Bressler[175], D.L. Briglin[19], T.M. Bristow[49], D. Britton[56], D. Britzger[45], F.M. Brochu[30], I. Brock[23], R. Brock[93], G. Brooijmans[38], T. Brooks[80], W.K. Brooks[34b], J. Brosamer[16], E. Brost[110], J.H Broughton[19], P.A. Bruckman de Renstrom[42], D. Bruncko[146b], A. Bruni[22a], G. Bruni[22a], L.S. Bruni[109], BH Brunt[30], M. Bruschi[22a], N. Bruscino[23], P. Bryant[33], L. Bryngemark[84], T. Buanes[15], Q. Buat[144], P. Buchholz[143], A.G. Buckley[56], I.A. Budagov[68], F. Buehrer[51], M.K. Bugge[121], O. Bulekov[100], D. Bullock[8], H. Burckhart[32], S. Burdin[77], C.D. Burgard[51], A.M. Burger[5], B. Burghgrave[110], K. Burka[42], S. Burke[133], I. Burmeister[46], J.T.P. Burr[122], E. Busato[37], D. Büscher[51], V. Büscher[86], P. Bussey[56], J.M. Butler[24], C.M. Buttar[56], J.M. Butterworth[81], P. Butti[32], W. Buttinger[27], A. Buzatu[35c], A.R. Buzykaev[111,c], S. Cabrera Urbán[170], D. Caforio[130], V.M. Cairo[40a,40b], O. Cakir[4a], N. Calace[52], P. Calafiura[16], A. Calandri[88], G. Calderini[83], P. Calfayan[64], G. Callea[40a,40b], L.P. Caloba[26a], S. Calvente Lopez[85], D. Calvet[37], S. Calvet[37], T.P. Calvet[88], R. Camacho Toro[33], S. Camarda[32], P. Camarri[135a,135b], D. Cameron[121], R. Caminal Armadans[169], C. Camincher[58], S. Campana[32], M. Campanelli[81], A. Camplani[94a,94b], A. Campoverde[143], V. Canale[106a,106b], M. Cano Bret[36c], J. Cantero[116], T. Cao[155], M.D.M. Capeans Garrido[32], I. Caprini[28b], M. Caprini[28b], M. Capua[40a,40b], R.M. Carbone[38], R. Cardarelli[135a], F. Cardillo[51], I. Carli[131], T. Carli[32], G. Carlino[106a], B.T. Carlson[127], L. Carminati[94a,94b], R.M.D. Carney[148a,148b], S. Caron[108], E. Carquin[34b], S. Carrá[94a,94b], G.D. Carrillo-Montoya[32], J. Carvalho[128a,128c], D. Casadei[19], M.P. Casado[13,j], M. Casolino[13], D.W. Casper[166], R. Castelijn[109], A. Castelli[109], V. Castillo Gimenez[170], N.F. Castro[128a,k], A. Catinaccio[32], J.R. Catmore[121], A. Cattai[32], J. Caudron[23], V. Cavaliere[169], E. Cavallaro[13], D. Cavalli[94a], M. Cavalli-Sforza[13], V. Cavasinni[126a,126b], E. Celebi[20a], F. Ceradini[136a,136b], L. Cerda Alberich[170], A.S. Cerqueira[26b], A. Cerri[151], L. Cerrito[135a,135b], F. Cerutti[16], A. Cervelli[18], S.A. Cetin[20d], A. Chafaq[137a], D. Chakraborty[110], S.K. Chan[59], W.S. Chan[109], Y.L. Chan[62a], P. Chang[169], J.D. Chapman[30], D.G. Charlton[19], A. Chatterjee[52], C.C. Chau[161], C.A. Chavez Barajas[151], S. Che[113], S. Cheatham[167a,167c], A. Chegwidden[93], S. Chekanov[6], S.V. Chekulaev[163a], G.A. Chelkov[68,l], M.A. Chelstowska[32], C. Chen[67], H. Chen[27], S. Chen[35b], S. Chen[157], X. Chen[35c,m], Y. Chen[70], H.C. Cheng[92], H.J. Cheng[35a], Y. Cheng[33], A. Cheplakov[68], E. Cheremushkina[132], R. Cherkaoui El Moursli[137e], V. Chernyatin[27,*], E. Cheu[7], L. Chevalier[138], V. Chiarella[50], G. Chiarelli[126a,126b], G. Chiodini[76a], A.S. Chisholm[32], A. Chitan[28b], Y.H. Chiu[172], M.V. Chizhov[68], K. Choi[64], A.R. Chomont[37], S. Chouridou[156], B.K.B. Chow[102], V. Christodoulou[81], D. Chromek-Burckhart[32], M.C. Chu[62a], J. Chudoba[129], A.J. Chuinard[90], J.J. Chwastowski[42], L. Chytka[117], A.K. Ciftci[4a], D. Cinca[46], V. Cindro[78], I.A. Cioara[23], C. Ciocca[22a,22b], A. Ciocio[16], F. Cirotto[106a,106b], Z.H. Citron[175], M. Citterio[94a], M. Ciubancan[28b], A. Clark[52], B.L. Clark[59], M.R. Clark[38], P.J. Clark[49], R.N. Clarke[16], C. Clement[148a,148b], Y. Coadou[88], M. Cobal[167a,167c], A. Coccaro[52], J. Cochran[67], L. Colasurdo[108], B. Cole[38], A.P. Colijn[109], J. Collot[58], T. Colombo[166], P. Conde Muiño[128a,128b], E. Coniavitis[51], S.H. Connell[147b], I.A. Connelly[87], V. Consorti[51], S. Constantinescu[28b], G. Conti[32], F. Conventi[106a,n], M. Cooke[16], B.D. Cooper[81], A.M. Cooper-Sarkar[122],



JHEP07(2017)107

F. Cormier[171], K.J.R. Cormier[161], M. Corradi[134a,134b], F. Corriveau[90,o], A. Cortes-Gonzalez[32], G. Cortiana[103], G. Costa[94a], M.J. Costa[170], D. Costanzo[141], G. Cottin[30], G. Cowan[80], B.E. Cox[87], K. Cranmer[112], S.J. Crawley[56], R.A. Creager[124], G. Cree[31], S. Crépé-Renaudin[58], F. Crescioli[83], W.A. Cribbs[148a,148b], M. Crispin Ortuzar[122], M. Cristinziani[23], V. Croft[108], G. Crosetti[40a,40b], A. Cueto[85], T. Cuhadar Donszelmann[141], A.R. Cukierman[145], J. Cummings[179], M. Curatolo[50], J. Cúth[86], H. Czirr[143], P. Czodrowski[32], G. D'amen[22a,22b], S. D'Auria[56], M. D'Onofrio[77], M.J. Da Cunha Sargedas De Sousa[128a,128b], C. Da Via[87], W. Dabrowski[41a], T. Dado[146a], T. Dai[92], O. Dale[15], F. Dallaire[97], C. Dallapiccola[89], M. Dam[39], J.R. Dandoy[124], N.P. Dang[51], A.C. Daniells[19], N.S. Dann[87], M. Danninger[171], M. Dano Hoffmann[138], V. Dao[150], G. Darbo[53a], S. Darmora[8], J. Dassoulas[3], A. Dattagupta[118], T. Daubney[45], W. Davey[23], C. David[45], T. Davidek[131], M. Davies[155], P. Davison[81], E. Dawe[91], I. Dawson[141], K. De[8], R. de Asmundis[106a], A. De Benedetti[115], S. De Castro[22a,22b], S. De Cecco[83], N. De Groot[108], P. de Jong[109], H. De la Torre[93], F. De Lorenzi[67], A. De Maria[57], D. De Pedis[134a], A. De Salvo[134a], U. De Sanctis[135a,135b], A. De Santo[151], K. De Vasconcelos Corga[88], J.B. De Vivie De Regie[119], W.J. Dearnaley[75], R. Debbe[27], C. Debenedetti[139], D.V. Dedovich[68], N. Dehghanian[3], I. Deigaard[109], M. Del Gaudio[40a,40b], J. Del Peso[85], T. Del Prete[126a,126b], D. Delgove[119], F. Deliot[138], C.M. Delitzsch[52], A. Dell'Acqua[32], L. Dell'Asta[24], M. Dell'Orso[126a,126b], M. Della Pietra[106a,106b], D. della Volpe[52], M. Delmastro[5], C. Delporte[119], P.A. Delsart[58], D.A. DeMarco[161], S. Demers[179], M. Demichev[68], A. Demilly[83], S.P. Denisov[132], D. Denysiuk[138], D. Derendarz[42], J.E. Derkaoui[137d], F. Derue[83], P. Dervan[77], K. Desch[23], C. Deterre[45], K. Dette[46], P.O. Deviveiros[32], A. Dewhurst[133], S. Dhaliwal[25], A. Di Ciaccio[135a,135b], L. Di Ciaccio[5], W.K. Di Clemente[124], C. Di Donato[106a,106b], A. Di Girolamo[32], B. Di Girolamo[32], B. Di Micco[136a,136b], R. Di Nardo[32], K.F. Di Petrillo[59], A. Di Simone[51], R. Di Sipio[161], D. Di Valentino[31], C. Diaconu[88], M. Diamond[161], F.A. Dias[49], M.A. Diaz[34a], E.B. Diehl[92], J. Dietrich[17], S. Díez Cornell[45], A. Dimitrievska[14], J. Dingfelder[23], P. Dita[28b], S. Dita[28b], F. Dittus[32], F. Djama[88], T. Djobava[54b], J.I. Djuvsland[60a], M.A.B. do Vale[26c], D. Dobos[32], M. Dobre[28b], C. Doglioni[84], J. Dolejsi[131], Z. Dolezal[131], M. Donadelli[26d], S. Donati[126a,126b], P. Dondero[123a,123b], J. Donini[37], J. Dopke[133], A. Doria[106a], M.T. Dova[74], A.T. Doyle[56], E. Drechsler[57], M. Dris[10], Y. Du[36b], J. Duarte-Campderros[155], E. Duchovni[175], G. Duckeck[102], A. Ducourthial[83], O.A. Ducu[97,p], D. Duda[109], A. Dudarev[32], A.Chr. Dudder[86], E.M. Duffield[16], L. Duflot[119], M. Dührssen[32], M. Dumancic[175], A.E. Dumitriu[28b], A.K. Duncan[56], M. Dunford[60a], H. Duran Yildiz[4a], M. Düren[55], A. Durglishvili[54b], D. Duschinger[47], B. Dutta[45], M. Dyndal[45], C. Eckardt[45], K.M. Ecker[103], R.C. Edgar[92], T. Eifert[32], G. Eigen[15], K. Einsweiler[16], T. Ekelof[168], M. El Kacimi[137c], R. El Kosseifi[88], V. Ellajosyula[88], M. Ellert[168], S. Elles[5], F. Ellinghaus[178], A.A. Elliot[172], N. Ellis[32], J. Elmsheuser[27], M. Elsing[32], D. Emeliyanov[133], Y. Enari[157], O.C. Endner[86], J.S. Ennis[173], J. Erdmann[46], A. Ereditato[18], G. Ernis[178], M. Ernst[27], S. Errede[169], E. Ertel[86], M. Escalier[119], H. Esch[46], C. Escobar[127], B. Esposito[50], O. Estrada Pastor[170], A.I. Etienvre[138], E. Etzion[155], H. Evans[64], A. Ezhilov[125], M. Ezzi[137e], F. Fabbri[22a,22b], L. Fabbri[22a,22b], G. Facini[33], R.M. Fakhrutdinov[132], S. Falciano[134a], R.J. Falla[81], J. Faltova[32], Y. Fang[35a], M. Fanti[94a,94b], A. Farbin[8], A. Farilla[136a], C. Farina[127], E.M. Farina[123a,123b], T. Farooque[93], S. Farrell[16], S.M. Farrington[173], P. Farthouat[32], F. Fassi[137e], P. Fassnacht[32], D. Fassouliotis[9], M. Faucci Giannelli[80], A. Favareto[53a,53b], W.J. Fawcett[122], L. Fayard[119], O.L. Fedin[125,q], W. Fedorko[171], S. Feigl[121], L. Feligioni[88], C. Feng[36b], E.J. Feng[32], H. Feng[92], A.B. Fenyuk[132], L. Feremenga[8], P. Fernandez Martinez[170], S. Fernandez Perez[13], J. Ferrando[45], A. Ferrari[168], P. Ferrari[109], R. Ferrari[123a], D.E. Ferreira de Lima[60b], A. Ferrer[170], D. Ferrere[52], C. Ferretti[92], F. Fiedler[86], A. Filipčič[78], M. Filipuzzi[45], F. Filthaut[108], M. Fincke-Keeler[172], K.D. Finelli[152], M.C.N. Fiolhais[128a,128c,r],



JHEP07(2017)107

L. Fiorini[170], A. Fischer[2], C. Fischer[13], J. Fischer[178], W.C. Fisher[93], N. Flaschel[45], I. Fleck[143], P. Fleischmann[92], R.R.M. Fletcher[124], T. Flick[178], B.M. Flierl[102], L.R. Flores Castillo[62a], M.J. Flowerdew[103], G.T. Forcolin[87], A. Formica[138], F.A. Förster[13], A. Forti[87], A.G. Foster[19], D. Fournier[119], H. Fox[75], S. Fracchia[141], P. Francavilla[83], M. Franchini[22a,22b], S. Franchino[60a], D. Francis[32], L. Franconi[121], M. Franklin[59], M. Frate[166], M. Fraternali[123a,123b], D. Freeborn[81], S.M. Fressard-Batraneanu[32], B. Freund[97], D. Froidevaux[32], J.A. Frost[122], C. Fukunaga[158], T. Fusayasu[104], J. Fuster[170], C. Gabaldon[58], O. Gabizon[154], A. Gabrielli[22a,22b], A. Gabrielli[16], G.P. Gach[41a], S. Gadatsch[32], S. Gadomski[80], G. Gagliardi[53a,53b], L.G. Gagnon[97], P. Gagnon[64], C. Galea[108], B. Galhardo[128a,128c], E.J. Gallas[122], B.J. Gallop[133], P. Gallus[130], G. Galster[39], K.K. Gan[113], S. Ganguly[37], J. Gao[36a], Y. Gao[77], Y.S. Gao[145,g], F.M. Garay Walls[49], C. García[170], J.E. García Navarro[170], M. Garcia-Sciveres[16], R.W. Gardner[33], N. Garelli[145], V. Garonne[121], A. Gascon Bravo[45], K. Gasnikova[45], C. Gatti[50], A. Gaudiello[53a,53b], G. Gaudio[123a], I.L. Gavrilenko[98], C. Gay[171], G. Gaycken[23], E.N. Gazis[10], C.N.P. Gee[133], M. Geisen[86], M.P. Geisler[60a], K. Gellerstedt[148a,148b], C. Gemme[53a], M.H. Genest[58], C. Geng[36a,s], S. Gentile[134a,134b], C. Gentsos[156], S. George[80], D. Gerbaudo[13], A. Gershon[155], S. Ghasemi[143], M. Ghneimat[23], B. Giacobbe[22a], S. Giagu[134a,134b], P. Giannetti[126a,126b], S.M. Gibson[80], M. Gignac[171], M. Gilchriese[16], D. Gillberg[31], G. Gilles[178], D.M. Gingrich[3,d], N. Giokaris[9,*], M.P. Giordani[167a,167c], F.M. Giorgi[22a], P.F. Giraud[138], P. Giromini[59], D. Giugni[94a], F. Giuli[122], C. Giuliani[103], M. Giulini[60b], B.K. Gjelsten[121], S. Gkaitatzis[156], I. Gkialas[9], E.L. Gkougkousis[139], L.K. Gladilin[101], C. Glasman[85], J. Glatzer[13], P.C.F. Glaysher[45], A. Glazov[45], M. Goblirsch-Kolb[25], J. Godlewski[42], S. Goldfarb[91], T. Golling[52], D. Golubkov[132], A. Gomes[128a,128b,128d], R. Gonçalo[128a], R. Goncalves Gama[26a], J. Goncalves Pinto Firmino Da Costa[138], G. Gonella[51], L. Gonella[19], A. Gongadze[68], S. González de la Hoz[170], S. Gonzalez-Sevilla[52], L. Goossens[32], P.A. Gorbounov[99], H.A. Gordon[27], I. Gorelov[107], B. Gorini[32], E. Gorini[76a,76b], A. Gorišek[78], A.T. Goshaw[48], C. Gössling[46], M.I. Gostkin[68], C.R. Goudet[119], D. Goujdami[137c], A.G. Goussiou[140], N. Govender[147b,t], E. Gozani[154], L. Graber[57], I. Grabowska-Bold[41a], P.O.J. Gradin[168], J. Gramling[52], E. Gramstad[121], S. Grancagnolo[17], V. Gratchev[125], P.M. Gravila[28f], C. Gray[56], H.M. Gray[32], Z.D. Greenwood[82,u], C. Grefe[23], K. Gregersen[81], I.M. Gregor[45], P. Grenier[145], K. Grevtsov[5], J. Griffiths[8], A.A. Grillo[139], K. Grimm[75], S. Grinstein[13,v], Ph. Gris[37], J.-F. Grivaz[119], S. Groh[86], E. Gross[175], J. Grosse-Knetter[57], G.C. Grossi[82], Z.J. Grout[81], A. Grummer[107], L. Guan[92], W. Guan[176], J. Guenther[65], F. Guescini[163a], D. Guest[166], O. Gueta[155], B. Gui[113], E. Guido[53a,53b], T. Guillemin[5], S. Guindon[2], U. Gul[56], C. Gumpert[32], J. Guo[36c], W. Guo[92], Y. Guo[36a], R. Gupta[43], S. Gupta[122], G. Gustavino[134a,134b], P. Gutierrez[115], N.G. Gutierrez Ortiz[81], C. Gutschow[81], C. Guyot[138], M.P. Guzik[41a], C. Gwenlan[122], C.B. Gwilliam[77], A. Haas[112], C. Haber[16], H.K. Hadavand[8], N. Haddad[137e], A. Hadef[88], S. Hageböck[23], M. Hagihara[164], H. Hakobyan[180,*], M. Haleem[45], J. Haley[116], G. Halladjian[93], G.D. Hallewell[88], K. Hamacher[178], P. Hamal[117], K. Hamano[172], A. Hamilton[147a], G.N. Hamity[141], P.G. Hamnett[45], L. Han[36a], S. Han[35a], K. Hanagaki[69,w], K. Hanawa[157], M. Hance[139], B. Haney[124], P. Hanke[60a], J.B. Hansen[39], J.D. Hansen[39], M.C. Hansen[23], P.H. Hansen[39], K. Hara[164], A.S. Hard[176], T. Harenberg[178], F. Hariri[119], S. Harkusha[95], R.D. Harrington[49], P.F. Harrison[173], N.M. Hartmann[102], M. Hasegawa[70], Y. Hasegawa[142], A. Hasib[49], S. Hassani[138], S. Haug[18], R. Hauser[93], L. Hauswald[47], L.B. Havener[38], M. Havranek[130], C.M. Hawkes[19], R.J. Hawkings[32], D. Hayakawa[159], D. Hayden[93], C.P. Hays[122], J.M. Hays[79], H.S. Hayward[77], S.J. Haywood[133], S.J. Head[19], T. Heck[86], V. Hedberg[84], L. Heelan[8], K.K. Heidegger[51], S. Heim[45], T. Heim[16], B. Heinemann[45,x], J.J. Heinrich[102], L. Heinrich[112], C. Heinz[55], J. Hejbal[129], L. Helary[32], A. Held[171], S. Hellman[148a,148b], C. Helsens[32], J. Henderson[122], R.C.W. Henderson[75], Y. Heng[176],



JHEP07(2017)107

S. Henkelmann[171], A.M. Henriques Correia[32], S. Henrot-Versille[119], G.H. Herbert[17], H. Herde[25], V. Herget[177], Y. Hernández Jiménez[147c], G. Herten[51], R. Hertenberger[102], L. Hervas[32], T.C. Herwig[124], G.G. Hesketh[81], N.P. Hessey[163a], J.W. Hetherly[43], S. Higashino[69], E. Higón-Rodriguez[170], E. Hill[172], J.C. Hill[30], K.H. Hiller[45], S.J. Hillier[19], I. Hinchliffe[16], M. Hirose[51], D. Hirschbuehl[178], B. Hiti[78], O. Hladik[129], X. Hoad[49], J. Hobbs[150], N. Hod[163a], M.C. Hodgkinson[141], P. Hodgson[141], A. Hoecker[32], M.R. Hoeferkamp[107], F. Hoenig[102], D. Hohn[23], T.R. Holmes[16], M. Homann[46], S. Honda[164], T. Honda[69], T.M. Hong[127], B.H. Hooberman[169], W.H. Hopkins[118], Y. Horii[105], A.J. Horton[144], J-Y. Hostachy[58], S. Hou[153], A. Hoummada[137a], J. Howarth[45], J. Hoya[74], M. Hrabovsky[117], I. Hristova[17], J. Hrivnac[119], T. Hryn'ova[5], A. Hrynevich[96], P.J. Hsu[63], S.-C. Hsu[140], Q. Hu[36a], S. Hu[36c], Y. Huang[35a], Z. Hubacek[130], F. Hubaut[88], F. Huegging[23], T.B. Huffman[122], E.W. Hughes[38], G. Hughes[75], M. Huhtinen[32], P. Huo[150], N. Huseynov[68,b], J. Huston[93], J. Huth[59], G. Iacobucci[52], G. Iakovidis[27], I. Ibragimov[143], L. Iconomidou-Fayard[119], Z. Idrissi[137e], P. Iengo[32], O. Igonkina[109,y], T. Iizawa[174], Y. Ikegami[69], M. Ikeno[69], Y. Ilchenko[11,z], D. Iliadis[156], N. Ilic[145], G. Introzzi[123a,123b], P. Ioannou[9,*], M. Iodice[136a], K. Iordanidou[38], V. Ippolito[59], M.F. Isacson[168], N. Ishijima[120], M. Ishino[157], M. Ishitsuka[159], C. Issever[122], S. Istin[20a], F. Ito[164], J.M. Iturbe Ponce[87], R. Iuppa[162a,162b], H. Iwasaki[69], J.M. Izen[44], V. Izzo[106a], S. Jabbar[3], P. Jackson[1], V. Jain[2], K.B. Jakobi[86], K. Jakobs[51], S. Jakobsen[32], T. Jakoubek[129], D.O. Jamin[116], D.K. Jana[82], R. Jansky[65], J. Janssen[23], M. Janus[57], P.A. Janus[41a], G. Jarlskog[84], N. Javadov[68,b], T. Javůrek[51], M. Javurkova[51], F. Jeanneau[138], L. Jeanty[16], J. Jejelava[54a,aa], A. Jelinskas[173], P. Jenni[51,ab], C. Jeske[173], S. Jézéquel[5], H. Ji[176], J. Jia[150], H. Jiang[67], Y. Jiang[36a], Z. Jiang[145], S. Jiggins[81], J. Jimenez Pena[170], S. Jin[35a], A. Jinaru[28b], O. Jinnouchi[159], H. Jivan[147c], P. Johansson[141], K.A. Johns[7], C.A. Johnson[64], W.J. Johnson[140], K. Jon-And[148a,148b], R.W.L. Jones[75], S.D. Jones[151], S. Jones[7], T.J. Jones[77], J. Jongmanns[60a], P.M. Jorge[128a,128b], J. Jovicevic[163a], X. Ju[176], A. Juste Rozas[13,v], M.K. Köhler[175], A. Kaczmarska[42], M. Kado[119], H. Kagan[113], M. Kagan[145], S.J. Kahn[88], T. Kaji[174], E. Kajomovitz[48], C.W. Kalderon[84], A. Kaluza[86], S. Kama[43], A. Kamenshchikov[132], N. Kanaya[157], S. Kaneti[30], L. Kanjir[78], V.A. Kantserov[100], J. Kanzaki[69], B. Kaplan[112], L.S. Kaplan[176], D. Kar[147c], K. Karakostas[10], N. Karastathis[10], M.J. Kareem[57], E. Karentzos[10], S.N. Karpov[68], Z.M. Karpova[68], K. Karthik[112], V. Kartvelishvili[75], A.N. Karyukhin[132], K. Kasahara[164], L. Kashif[176], R.D. Kass[113], A. Kastanas[149], Y. Kataoka[157], C. Kato[157], A. Katre[52], J. Katzy[45], K. Kawade[105], K. Kawagoe[73], T. Kawamoto[157], G. Kawamura[57], E.F. Kay[77], V.F. Kazanin[111,c], R. Keeler[172], R. Kehoe[43], J.S. Keller[45], J.J. Kempster[80], H. Keoshkerian[161], O. Kepka[129], B.P. Kerševan[78], S. Kersten[178], R.A. Keyes[90], M. Khader[169], F. Khalil-zada[12], A. Khanov[116], A.G. Kharlamov[111,c], T. Kharlamova[111,c], A. Khodinov[160], T.J. Khoo[52], V. Khovanskiy[99,*], E. Khramov[68], J. Khubua[54b,ac], S. Kido[70], C.R. Kilby[80], H.Y. Kim[8], S.H. Kim[164], Y.K. Kim[33], N. Kimura[156], O.M. Kind[17], B.T. King[77], D. Kirchmeier[47], J. Kirk[133], A.E. Kiryunin[103], T. Kishimoto[157], D. Kisielewska[41a], K. Kiuchi[164], O. Kivernyk[5], E. Kladiva[146b], T. Klapdor-Kleingrothaus[51], M.H. Klein[38], M. Klein[77], U. Klein[77], K. Kleinknecht[86], P. Klimek[110], A. Klimentov[27], R. Klingenberg[46], T. Klingl[23], T. Klioutchnikova[32], E.-E. Kluge[60a], P. Kluit[109], S. Kluth[103], J. Knapik[42], E. Kneringer[65], E.B.F.G. Knoops[88], A. Knue[103], A. Kobayashi[157], D. Kobayashi[159], T. Kobayashi[157], M. Kobel[47], M. Kocian[145], P. Kodys[131], T. Koffas[31], E. Koffeman[109], N.M. Köhler[103], T. Koi[145], M. Kolb[60b], I. Koletsou[5], A.A. Komar[98,*], Y. Komori[157], T. Kondo[69], N. Kondrashova[36c], K. Köneke[51], A.C. König[108], T. Kono[69,ad], R. Konoplich[112,ae], N. Konstantinidis[81], R. Kopeliansky[64], S. Koperny[41a], A.K. Kopp[51], K. Korcyl[42], K. Kordas[156], A. Korn[81], A.A. Korol[111,c], I. Korolkov[13], E.V. Korolkova[141], O. Kortner[103], S. Kortner[103], T. Kosek[131], V.V. Kostyukhin[23], A. Kotwal[48], A. Koulouris[10], A. Kourkoumeli-Charalampidi[123a,123b], C. Kourkoumelis[9], E. Kourlitis[141],



JHEP07(2017)107

V. Kouskoura[27], A.B. Kowalewska[42], R. Kowalewski[172], T.Z. Kowalski[41a], C. Kozakai[157], W. Kozanecki[138], A.S. Kozhin[132], V.A. Kramarenko[101], G. Kramberger[78], D. Krasnopevtsev[100], M.W. Krasny[83], A. Krasznahorkay[32], D. Krauss[103], A. Kravchenko[27], J.A. Kremer[41a], M. Kretz[60c], J. Kretzschmar[77], K. Kreutzfeldt[55], P. Krieger[161], K. Krizka[33], K. Kroeninger[46], H. Kroha[103], J. Kroll[129], J. Kroll[124], J. Kroseberg[23], J. Krstic[14], U. Kruchonak[68], H. Krüger[23], N. Krumnack[67], M.C. Kruse[48], M. Kruskal[24], T. Kubota[91], H. Kucuk[81], S. Kuday[4b], J.T. Kuechler[178], S. Kuehn[32], A. Kugel[60c], F. Kuger[177], T. Kuhl[45], V. Kukhtin[68], R. Kukla[88], Y. Kulchitsky[95], S. Kuleshov[34b], Y.P. Kulinich[169], M. Kuna[134a,134b], T. Kunigo[71], A. Kupco[129], O. Kuprash[155], H. Kurashige[70], L.L. Kurchaninov[163a], Y.A. Kurochkin[95], M.G. Kurth[35a], V. Kus[129], E.S. Kuwertz[172], M. Kuze[159], J. Kvita[117], T. Kwan[172], D. Kyriazopoulos[141], A. La Rosa[103], J.L. La Rosa Navarro[26d], L. La Rotonda[40a,40b], C. Lacasta[170], F. Lacava[134a,134b], J. Lacey[45], H. Lacker[17], D. Lacour[83], E. Ladygin[68], R. Lafaye[5], B. Laforge[83], T. Lagouri[179], S. Lai[57], S. Lammers[64], W. Lampl[7], E. Lançon[27], U. Landgraf[51], M.P.J. Landon[79], M.C. Lanfermann[52], V.S. Lang[60a], J.C. Lange[13], A.J. Lankford[166], F. Lanni[27], K. Lantzsch[23], A. Lanza[123a], A. Lapertosa[53a,53b], S. Laplace[83], J.F. Laporte[138], T. Lari[94a], F. Lasagni Manghi[22a,22b], M. Lassnig[32], P. Laurelli[50], W. Lavrijsen[16], A.T. Law[139], P. Laycock[77], T. Lazovich[59], M. Lazzaroni[94a,94b], B. Le[91], O. Le Dortz[83], E. Le Guirriec[88], E.P. Le Quilleuc[138], M. LeBlanc[172], T. LeCompte[6], F. Ledroit-Guillon[58], C.A. Lee[27], G.R. Lee[133,af], S.C. Lee[153], L. Lee[59], B. Lefebvre[90], G. Lefebvre[83], M. Lefebvre[172], F. Legger[102], C. Leggett[16], A. Lehan[77], G. Lehmann Miotto[32], X. Lei[7], W.A. Leight[45], M.A.L. Leite[26d], R. Leitner[131], D. Lellouch[175], B. Lemmer[57], K.J.C. Leney[81], T. Lenz[23], B. Lenzi[32], R. Leone[7], S. Leone[126a,126b], C. Leonidopoulos[49], G. Lerner[151], C. Leroy[97], A.A.J. Lesage[138], C.G. Lester[30], M. Levchenko[125], J. Levêque[5], D. Levin[92], L.J. Levinson[175], M. Levy[19], D. Lewis[79], B. Li[36a,s], C. Li[36a], H. Li[150], L. Li[36c], Q. Li[35a], S. Li[48], X. Li[36c], Y. Li[143], Z. Liang[35a], B. Liberti[135a], A. Liblong[161], K. Lie[62c], J. Liebal[23], W. Liebig[15], A. Limosani[152], S.C. Lin[153,ag], T.H. Lin[86], B.E. Lindquist[150], A.E. Lionti[52], E. Lipeles[124], A. Lipniacka[15], M. Lisovyi[60b], T.M. Liss[169], A. Lister[171], A.M. Litke[139], B. Liu[153,ah], H. Liu[92], H. Liu[27], J.K.K. Liu[122], J. Liu[36b], J.B. Liu[36a], K. Liu[88], L. Liu[169], M. Liu[36a], Y.L. Liu[36a], Y. Liu[36a], M. Livan[123a,123b], A. Lleres[58], J. Llorente Merino[35a], S.L. Lloyd[79], C.Y. Lo[62b], F. Lo Sterzo[153], E.M. Lobodzinska[45], P. Loch[7], F.K. Loebinger[87], K.M. Loew[25], A. Loginov[179,*], T. Lohse[17], K. Lohwasser[45], M. Lokajicek[129], B.A. Long[24], J.D. Long[169], R.E. Long[75], L. Longo[76a,76b], K.A. Looper[113], J.A. Lopez[34b], D. Lopez Mateos[59], I. Lopez Paz[13], A. Lopez Solis[83], J. Lorenz[102], N. Lorenzo Martinez[5], M. Losada[21], P.J. Lösel[102], X. Lou[35a], A. Lounis[119], J. Love[6], P.A. Love[75], H. Lu[62a], N. Lu[92], Y.J. Lu[63], H.J. Lubatti[140], C. Luci[134a,134b], A. Lucotte[58], C. Luedtke[51], F. Luehring[64], W. Lukas[65], L. Luminari[134a], O. Lundberg[148a,148b], B. Lund-Jensen[149], P.M. Luzi[83], D. Lynn[27], R. Lysak[129], E. Lytken[84], V. Lyubushkin[68], H. Ma[27], L.L. Ma[36b], Y. Ma[36b], G. Maccarrone[50], A. Macchiolo[103], C.M. Macdonald[141], B. Maček[78], J. Machado Miguens[124,128b], D. Madaffari[88], R. Madar[37], H.J. Maddocks[168], W.F. Mader[47], A. Madsen[45], J. Maeda[70], S. Maeland[15], T. Maeno[27], A.S. Maevskiy[101], E. Magradze[57], J. Mahlstedt[109], C. Maiani[119], C. Maidantchik[26a], A.A. Maier[103], T. Maier[102], A. Maio[128a,128b,128d], S. Majewski[118], Y. Makida[69], N. Makovec[119], B. Malaescu[83], Pa. Malecki[42], V.P. Maleev[125], F. Malek[58], U. Mallik[66], D. Malon[6], C. Malone[30], S. Maltezos[10], S. Malyukov[32], J. Mamuzic[170], G. Mancini[50], L. Mandelli[94a], I. Mandić[78], J. Maneira[128a,128b], L. Manhaes de Andrade Filho[26b], J. Manjarres Ramos[163b], A. Mann[102], A. Manousos[32], B. Mansoulie[138], J.D. Mansour[35a], R. Mantifel[90], M. Mantoani[57], S. Manzoni[94a,94b], L. Mapelli[32], G. Marceca[29], L. March[52], L. Marchese[122], G. Marchiori[83], M. Marcisovsky[129], M. Marjanovic[37], D.E. Marley[92], F. Marroquim[26a], S.P. Marsden[87], Z. Marshall[16], M.U.F Martensson[168], S. Marti-Garcia[170], C.B. Martin[113], T.A. Martin[173], V.J. Martin[49], B. Martin dit Latour[15], M. Martinez[13,v],



JHEP07(2017)107

V.I. Martinez Outschoorn[169], S. Martin-Haugh[133], V.S. Martoiu[28b], A.C. Martyniuk[81], A. Marzin[32], L. Masetti[86], T. Mashimo[157], R. Mashinistov[98], J. Masik[87], A.L. Maslennikov[111,c], L. Massa[135a,135b], P. Mastrandrea[5], A. Mastroberardino[40a,40b], T. Masubuchi[157], P. Mättig[178], J. Maurer[28b], S.J. Maxfield[77], D.A. Maximov[111,c], R. Mazini[153], I. Maznas[156], S.M. Mazza[94a,94b], N.C. Mc Fadden[107], G. Mc Goldrick[161], S.P. Mc Kee[92], A. McCarn[92], R.L. McCarthy[150], T.G. McCarthy[103], L.I. McClymont[81], E.F. McDonald[91], J.A. Mcfayden[81], G. Mchedlidze[57], S.J. McMahon[133], P.C. McNamara[91], R.A. McPherson[172,o], S. Meehan[140], T.J. Megy[51], S. Mehlhase[102], A. Mehta[77], T. Meideck[58], K. Meier[60a], C. Meineck[102], B. Meirose[44], D. Melini[170,ai], B.R. Mellado Garcia[147c], M. Melo[146a], F. Meloni[18], S.B. Menary[87], L. Meng[77], X.T. Meng[92], A. Mengarelli[22a,22b], S. Menke[103], E. Meoni[40a,40b], S. Mergelmeyer[17], P. Mermod[52], L. Merola[106a,106b], C. Meroni[94a], F.S. Merritt[33], A. Messina[134a,134b], J. Metcalfe[6], A.S. Mete[166], C. Meyer[124], J-P. Meyer[138], J. Meyer[109], H. Meyer Zu Theenhausen[60a], F. Miano[151], R.P. Middleton[133], S. Miglioranzi[53a,53b], L. Mijović[49], G. Mikenberg[175], M. Mikestikova[129], M. Mikuž[78], M. Milesi[91], A. Milic[27], D.W. Miller[33], C. Mills[49], A. Milov[175], D.A. Milstead[148a,148b], A.A. Minaenko[132], Y. Minami[157], I.A. Minashvili[68], A.I. Mincer[112], B. Mindur[41a], M. Mineev[68], Y. Minegishi[157], Y. Ming[176], L.M. Mir[13], K.P. Mistry[124], T. Mitani[174], J. Mitrevski[102], V.A. Mitsou[170], A. Miucci[18], P.S. Miyagawa[141], A. Mizukami[69], J.U. Mjörnmark[84], M. Mlynarikova[131], T. Moa[148a,148b], K. Mochizuki[97], P. Mogg[51], S. Mohapatra[38], S. Molander[148a,148b], R. Moles-Valls[23], R. Monden[71], M.C. Mondragon[93], K. Mönig[45], J. Monk[39], E. Monnier[88], A. Montalbano[150], J. Montejo Berlingen[32], F. Monticelli[74], S. Monzani[94a,94b], R.W. Moore[3], N. Morange[119], D. Moreno[21], M. Moreno Llácer[57], P. Morettini[53a], S. Morgenstern[32], D. Mori[144], T. Mori[157], M. Morii[59], M. Morinaga[157], V. Morisbak[121], A.K. Morley[152], G. Mornacchi[32], J.D. Morris[79], L. Morvaj[150], P. Moschovakos[10], M. Mosidze[54b], H.J. Moss[141], J. Moss[145,aj], K. Motohashi[159], R. Mount[145], E. Mountricha[27], E.J.W. Moyse[89], S. Muanza[88], R.D. Mudd[19], F. Mueller[103], J. Mueller[127], R.S.P. Mueller[102], D. Muenstermann[75], P. Mullen[56], G.A. Mullier[18], F.J. Munoz Sanchez[87], W.J. Murray[173,133], H. Musheghyan[181], M. Muškinja[78], A.G. Myagkov[132,ak], M. Myska[130], B.P. Nachman[16], O. Nackenhorst[52], K. Nagai[122], R. Nagai[69,ad], K. Nagano[69], Y. Nagasaka[61], K. Nagata[164], M. Nagel[51], E. Nagy[88], A.M. Nairz[32], Y. Nakahama[105], K. Nakamura[69], T. Nakamura[157], I. Nakano[114], R.F. Naranjo Garcia[45], R. Narayan[11], D.I. Narrias Villar[60a], I. Naryshkin[125], T. Naumann[45], G. Navarro[21], R. Nayyar[7], H.A. Neal[92], P.Yu. Nechaeva[98], T.J. Neep[138], A. Negri[123a,123b], M. Negrini[22a], S. Nektarijevic[108], C. Nellist[119], A. Nelson[166], M.E. Nelson[122], S. Nemecek[129], P. Nemethy[112], A.A. Nepomuceno[26a], M. Nessi[32,al], M.S. Neubauer[169], M. Neumann[178], P.R. Newman[19], T.Y. Ng[62c], T. Nguyen Manh[97], R.B. Nickerson[122], R. Nicolaidou[138], J. Nielsen[139], V. Nikolaenko[132,ak], I. Nikolic-Audit[83], K. Nikolopoulos[19], J.K. Nilsen[121], P. Nilsson[27], Y. Ninomiya[157], A. Nisati[134a], N. Nishu[35c], R. Nisius[103], T. Nobe[157], Y. Noguchi[71], M. Nomachi[120], I. Nomidis[31], M.A. Nomura[27], T. Nooney[79], M. Nordberg[32], N. Norjoharuddeen[122], O. Novgorodova[47], S. Nowak[103], M. Nozaki[69], L. Nozka[117], K. Ntekas[166], E. Nurse[81], F. Nuti[91], K. O'connor[25], D.C. O'Neil[144], A.A. O'Rourke[45], V. O'Shea[56], F.G. Oakham[31,d], H. Oberlack[103], T. Obermann[23], J. Ocariz[83], A. Ochi[70], I. Ochoa[38], J.P. Ochoa-Ricoux[34a], S. Oda[73], S. Odaka[69], H. Ogren[64], A. Oh[87], S.H. Oh[48], C.C. Ohm[16], H. Ohman[168], H. Oide[53a,53b], H. Okawa[164], Y. Okumura[157], T. Okuyama[69], A. Olariu[28b], L.F. Oleiro Seabra[128a], S.A. Olivares Pino[49], D. Oliveira Damazio[27], A. Olszewski[42], J. Olszowska[42], A. Onofre[128a,128e], K. Onogi[105], P.U.E. Onyisi[11,z], M.J. Oreglia[33], Y. Oren[155], D. Orestano[136a,136b], N. Orlando[62b], R.S. Orr[161], B. Osculati[53a,53b,*], R. Ospanov[87], G. Otero y Garzon[29], H. Otono[73], M. Ouchrif[137d], F. Ould-Saada[121], A. Ouraou[138], K.P. Oussoren[109], Q. Ouyang[35a], M. Owen[56], R.E. Owen[19], V.E. Ozcan[20a], N. Ozturk[8], K. Pachal[144], A. Pacheco Pages[13], L. Pacheco Rodriguez[138],



JHEP07(2017)107

C. Padilla Aranda[13], S. Pagan Griso[16], M. Paganini[179], F. Paige[27], P. Pais[89], G. Palacino[64], S. Palazzo[40a,40b], S. Palestini[32], M. Palka[41b], D. Pallin[37], E.St. Panagiotopoulou[10], I. Panagoulias[10], C.E. Pandini[83], J.G. Panduro Vazquez[80], P. Pani[32], S. Panitkin[27], D. Pantea[28b], L. Paolozzi[52], Th.D. Papadopoulou[10], K. Papageorgiou[9], A. Paramonov[6], D. Paredes Hernandez[179], A.J. Parker[75], M.A. Parker[30], K.A. Parker[45], F. Parodi[53a,53b], J.A. Parsons[38], U. Parzefall[51], V.R. Pascuzzi[161], J.M. Pasner[139], E. Pasqualucci[134a], S. Passaggio[53a], Fr. Pastore[80], S. Pataraia[178], J.R. Pater[87], T. Pauly[32], J. Pearce[172], B. Pearson[103], S. Pedraza Lopez[170], R. Pedro[128a,128b], S.V. Peleganchuk[111,c], O. Penc[129], C. Peng[35a], H. Peng[36a], J. Penwell[64], B.S. Peralva[26b], M.M. Perego[138], D.V. Perepelitsa[27], L. Perini[94a,94b], H. Pernegger[32], S. Perrella[106a,106b], R. Peschke[45], V.D. Peshekhonov[68,*], K. Peters[45], R.F.Y. Peters[87], B.A. Petersen[32], T.C. Petersen[39], E. Petit[58], A. Petridis[1], C. Petridou[156], P. Petroff[119], E. Petrolo[134a], M. Petrov[122], F. Petrucci[136a,136b], N.E. Pettersson[89], A. Peyaud[138], R. Pezoa[34b], F.H. Phillips[93], P.W. Phillips[133], G. Piacquadio[150], E. Pianori[173], A. Picazio[89], E. Piccaro[79], M.A. Pickering[122], R. Piegaia[29], J.E. Pilcher[33], A.D. Pilkington[87], A.W.J. Pin[87], M. Pinamonti[135a,135b], J.L. Pinfold[3], H. Pirumov[45], M. Pitt[175], L. Plazak[146a], M.-A. Pleier[27], V. Pleskot[86], E. Plotnikova[68], D. Pluth[67], P. Podberezko[111], R. Poettgen[148a,148b], R. Poggi[123a,123b], L. Poggioli[119], D. Pohl[23], G. Polesello[123a], A. Poley[45], A. Policicchio[40a,40b], R. Polifka[32], A. Polini[22a], C.S. Pollard[56], V. Polychronakos[27], K. Pommès[32], D. Ponomarenko[100], L. Pontecorvo[134a], B.G. Pope[93], G.A. Popeneciu[28d], A. Poppleton[32], S. Pospisil[130], K. Potamianos[16], I.N. Potrap[68], C.J. Potter[30], G. Poulard[32], J. Poveda[32], M.E. Pozo Astigarraga[32], P. Pralavorio[88], A. Pranko[16], S. Prell[67], D. Price[87], L.E. Price[6], M. Primavera[76a], S. Prince[90], N. Proklova[100], K. Prokofiev[62c], F. Prokoshin[34b], S. Protopopescu[27], J. Proudfoot[6], M. Przybycien[41a], D. Puddu[136a,136b], A. Puri[169], P. Puzo[119], J. Qian[92], G. Qin[56], Y. Qin[87], A. Quadt[57], M. Queitsch-Maitland[45], D. Quilty[56], S. Raddum[121], V. Radeka[27], V. Radescu[122], S.K. Radhakrishnan[150], P. Radloff[118], P. Rados[91], F. Ragusa[94a,94b], G. Rahal[182], J.A. Raine[87], S. Rajagopalan[27], C. Rangel-Smith[168], T. Rashid[119], M.G. Ratti[94a,94b], D.M. Rauch[45], F. Rauscher[102], S. Rave[86], T. Ravenscroft[56], I. Ravinovich[175], J.H. Rawling[87], M. Raymond[32], A.L. Read[121], N.P. Readioff[77], M. Reale[76a,76b], D.M. Rebuzzi[123a,123b], A. Redelbach[177], G. Redlinger[27], R. Reece[139], R.G. Reed[147c], K. Reeves[44], L. Rehnisch[17], J. Reichert[124], A. Reiss[86], C. Rembser[32], H. Ren[35a], M. Rescigno[134a], S. Resconi[94a], E.D. Resseguie[124], S. Rettie[171], E. Reynolds[19], O.L. Rezanova[111,c], P. Reznicek[131], R. Rezvani[97], R. Richter[103], S. Richter[81], E. Richter-Was[41b], O. Ricken[23], M. Ridel[83], P. Rieck[103], C.J. Riegel[178], J. Rieger[57], O. Rifki[115], M. Rijssenbeek[150], A. Rimoldi[123a,123b], M. Rimoldi[18], L. Rinaldi[22a], B. Ristić[52], E. Ritsch[32], I. Riu[13], F. Rizatdinova[116], E. Rizvi[79], C. Rizzi[13], R.T. Roberts[87], S.H. Robertson[90,o], A. Robichaud-Veronneau[90], D. Robinson[30], J.E.M. Robinson[45], A. Robson[56], E. Rocco[86], C. Roda[126a,126b], Y. Rodina[88,am], S. Rodriguez Bosca[170], A. Rodriguez Perez[13], D. Rodriguez Rodriguez[170], S. Roe[32], C.S. Rogan[59], O. Røhne[121], J. Roloff[59], A. Romaniouk[100], M. Romano[22a,22b], S.M. Romano Saez[37], E. Romero Adam[170], N. Rompotis[77], M. Ronzani[51], L. Roos[83], S. Rosati[134a], K. Rosbach[51], P. Rose[139], N.-A. Rosien[57], V. Rossetti[148a,148b], E. Rossi[106a,106b], L.P. Rossi[53a], J.H.N. Rosten[30], R. Rosten[140], M. Rotaru[28b], I. Roth[175], J. Rothberg[140], D. Rousseau[119], A. Rozanov[88], Y. Rozen[154], X. Ruan[147c], F. Rubbo[145], F. Rühr[51], A. Ruiz-Martinez[31], Z. Rurikova[51], N.A. Rusakovich[68], H.L. Russell[140], J.P. Rutherfoord[7], N. Ruthmann[32], Y.F. Ryabov[125], M. Rybar[169], G. Rybkin[119], S. Ryu[6], A. Ryzhov[132], G.F. Rzehorz[57], A.F. Saavedra[152], G. Sabato[109], S. Sacerdoti[29], H.F-W. Sadrozinski[139], R. Sadykov[68], F. Safai Tehrani[134a], P. Saha[110], M. Sahinsoy[60a], M. Saimpert[45], M. Saito[157], T. Saito[157], H. Sakamoto[157], Y. Sakurai[174], G. Salamanna[136a,136b], J.E. Salazar Loyola[34b], D. Salek[109], P.H. Sales De Bruin[168], D. Salihagic[103], A. Salnikov[145],



JHEP07(2017)107

J. Salt[170], D. Salvatore[40a,40b], F. Salvatore[151], A. Salvucci[62a,62b,62c], A. Salzburger[32], D. Sammel[51], D. Sampsonidis[156], D. Sampsonidou[156], J. Sánchez[170], V. Sanchez Martinez[170], A. Sanchez Pineda[167a,167c], H. Sandaker[121], R.L. Sandbach[79], C.O. Sander[45], M. Sandhoff[178], C. Sandoval[21], D.P.C. Sankey[133], M. Sannino[53a,53b], A. Sansoni[50], C. Santoni[37], R. Santonico[135a,135b], H. Santos[128a], I. Santoyo Castillo[151], K. Sapp[127], A. Sapronov[68], J.G. Saraiva[128a,128d], B. Sarrazin[23], O. Sasaki[69], K. Sato[164], E. Sauvan[5], G. Savage[80], P. Savard[161,d], N. Savic[103], C. Sawyer[133], L. Sawyer[82,u], J. Saxon[33], C. Sbarra[22a], A. Sbrizzi[22a,22b], T. Scanlon[81], D.A. Scannicchio[166], M. Scarcella[152], V. Scarfone[40a,40b], J. Schaarschmidt[140], P. Schacht[103], B.M. Schachtner[102], D. Schaefer[32], L. Schaefer[124], R. Schaefer[45], J. Schaeffer[86], S. Schaepe[23], S. Schaetzel[60b], U. Schäfer[86], A.C. Schaffer[119], D. Schaile[102], R.D. Schamberger[150], V. Scharf[60a], V.A. Schegelsky[125], D. Scheirich[131], M. Schernau[166], C. Schiavi[53a,53b], S. Schier[139], L.K. Schildgen[23], C. Schillo[51], M. Schioppa[40a,40b], S. Schlenker[32], K.R. Schmidt-Sommerfeld[103], K. Schmieden[32], C. Schmitt[86], S. Schmitt[45], S. Schmitz[86], U. Schnoor[51], L. Schoeffel[138], A. Schoening[60b], B.D. Schoenrock[93], E. Schopf[23], M. Schott[86], J.F.P. Schouwenberg[108], J. Schovancova[181], S. Schramm[52], N. Schuh[86], A. Schulte[86], M.J. Schultens[23], H.-C. Schultz-Coulon[60a], H. Schulz[17], M. Schumacher[51], B.A. Schumm[139], Ph. Schune[138], A. Schwartzman[145], T.A. Schwarz[92], H. Schweiger[87], Ph. Schwemling[138], R. Schwienhorst[93], J. Schwindling[138], T. Schwindt[23], A. Sciandra[23], G. Sciolla[25], F. Scuri[126a,126b], F. Scutti[91], J. Searcy[92], P. Seema[23], S.C. Seidel[107], A. Seiden[139], J.M. Seixas[26a], G. Sekhniaidze[106a], K. Sekhon[92], S.J. Sekula[43], N. Semprini-Cesari[22a,22b], S. Senkin[37], C. Serfon[121], L. Serin[119], L. Serkin[167a,167b], M. Sessa[136a,136b], R. Seuster[172], H. Severini[115], T. Sfiligoj[78], F. Sforza[32], A. Sfyrla[52], E. Shabalina[57], N.W. Shaikh[148a,148b], L.Y. Shan[35a], R. Shang[169], J.T. Shank[24], M. Shapiro[16], P.B. Shatalov[99], K. Shaw[167a,167b], S.M. Shaw[87], A. Shcherbakova[148a,148b], C.Y. Shehu[151], Y. Shen[115], P. Sherwood[81], L. Shi[153,an], S. Shimizu[70], C.O. Shimmin[179], M. Shimojima[104], I.P.J. Shipsey[122], S. Shirabe[73], M. Shiyakova[68,ao], J. Shlomi[175], A. Shmeleva[98], D. Shoaleh Saadi[97], M.J. Shochet[33], S. Shojaii[94a], D.R. Shope[115], S. Shrestha[113], E. Shulga[100], M.A. Shupe[7], P. Sicho[129], A.M. Sickles[169], P.E. Sidebo[149], E. Sideras Haddad[147c], O. Sidiropoulou[177], D. Sidorov[116], A. Sidoti[22a,22b], F. Siegert[47], Dj. Sijacki[14], J. Silva[128a,128d], S.B. Silverstein[148a], V. Simak[130], Lj. Simic[14], S. Simion[119], E. Simioni[86], B. Simmons[81], M. Simon[86], P. Sinervo[161], N.B. Sinev[118], M. Sioli[22a,22b], G. Siragusa[177], I. Siral[92], S.Yu. Sivoklokov[101], J. Sjölin[148a,148b], M.B. Skinner[75], P. Skubic[115], M. Slater[19], T. Slavicek[130], M. Slawinska[109], K. Sliwa[165], R. Slovak[131], V. Smakhtin[175], B.H. Smart[5], J. Smiesko[146a], N. Smirnov[100], S.Yu. Smirnov[100], Y. Smirnov[100], L.N. Smirnova[101,ap], O. Smirnova[84], J.W. Smith[57], M.N.K. Smith[38], R.W. Smith[38], M. Smizanska[75], K. Smolek[130], A.A. Snesarev[98], I.M. Snyder[118], S. Snyder[27], R. Sobie[172,o], F. Socher[47], A. Soffer[155], D.A. Soh[153], G. Sokhrannyi[78], C.A. Solans Sanchez[32], M. Solar[130], E.Yu. Soldatov[100], U. Soldevila[170], A.A. Solodkov[132], A. Soloshenko[68], O.V. Solovyanov[132], V. Solovyev[125], P. Sommer[51], H. Son[165], H.Y. Song[36a,aq], A. Sopczak[130], D. Sosa[60b], C.L. Sotiropoulou[126a,126b], R. Soualah[167a,167c], A.M. Soukharev[111,c], D. South[45], B.C. Sowden[80], S. Spagnolo[76a,76b], M. Spalla[126a,126b], M. Spangenberg[173], F. Spanò[80], D. Sperlich[17], F. Spettel[103], T.M. Spieker[60a], R. Spighi[22a], G. Spigo[32], L.A. Spiller[91], M. Spousta[131], R.D. St. Denis[56,*], A. Stabile[94a], R. Stamen[60a], S. Stamm[17], E. Stanecka[42], R.W. Stanek[6], C. Stanescu[136a], M.M. Stanitzki[45], S. Stapnes[121], E.A. Starchenko[132], G.H. Stark[33], J. Stark[58], S.H Stark[39], P. Staroba[129], P. Starovoitov[60a], S. Stärz[32], R. Staszewski[42], P. Steinberg[27], B. Stelzer[144], H.J. Stelzer[32], O. Stelzer-Chilton[163a], H. Stenzel[55], G.A. Stewart[56], M.C. Stockton[118], M. Stoebe[90], G. Stoicea[28b], P. Stolte[57], S. Stonjek[103], A.R. Stradling[8], A. Straessner[47], M.E. Stramaglia[18], J. Strandberg[149], S. Strandberg[148a,148b], A. Strandlie[121], M. Strauss[115], P. Strizenec[146b], R. Ströhmer[177], D.M. Strom[118], R. Stroynowski[43], A. Strubig[108],



JHEP07(2017)107

S.A. Stucci[27], B. Stugu[15], N.A. Styles[45], D. Su[145], J. Su[127], S. Suchek[60a], Y. Sugaya[120], M. Suk[130], V.V. Sulin[98], S. Sultansoy[4c], T. Sumida[71], S. Sun[59], X. Sun[3], K. Suruliz[151], C.J.E. Suster[152], M.R. Sutton[151], S. Suzuki[69], M. Svatos[129], M. Swiatlowski[33], S.P. Swift[2], I. Sykora[146a], T. Sykora[131], D. Ta[51], K. Tackmann[45], J. Taenzer[155], A. Taffard[166], R. Tafirout[163a], N. Taiblum[155], H. Takai[27], R. Takashima[72], T. Takeshita[142], Y. Takubo[69], M. Talby[88], A.A. Talyshev[111,c], J. Tanaka[157], M. Tanaka[159], R. Tanaka[119], S. Tanaka[69], R. Tanioka[70], B.B. Tannenwald[113], S. Tapia Araya[34b], S. Tapprogge[86], S. Tarem[154], G.F. Tartarelli[94a], P. Tas[131], M. Tasevsky[129], T. Tashiro[71], E. Tassi[40a,40b], A. Tavares Delgado[128a,128b], Y. Tayalati[137e], A.C. Taylor[107], G.N. Taylor[91], P.T.E. Taylor[91], W. Taylor[163b], P. Teixeira-Dias[80], D. Temple[144], H. Ten Kate[32], P.K. Teng[153], J.J. Teoh[120], F. Tepel[178], S. Terada[69], K. Terashi[157], J. Terron[85], S. Terzo[13], M. Testa[50], R.J. Teuscher[161,o], T. Theveneaux-Pelzer[88], J.P. Thomas[19], J. Thomas-Wilsker[80], P.D. Thompson[19], A.S. Thompson[56], L.A. Thomsen[179], E. Thomson[124], M.J. Tibbetts[16], R.E. Ticse Torres[88], V.O. Tikhomirov[98,ar], Yu.A. Tikhonov[111,c], S. Timoshenko[100], P. Tipton[179], S. Tisserant[88], K. Todome[159], S. Todorova-Nova[5], J. Tojo[73], S. Tokár[146a], K. Tokushuku[69], E. Tolley[59], L. Tomlinson[87], M. Tomoto[105], L. Tompkins[145,as], K. Toms[107], B. Tong[59], P. Tornambe[51], E. Torrence[118], H. Torres[144], E. Torró Pastor[140], J. Toth[88,at], F. Touchard[88], D.R. Tovey[141], C.J. Treado[112], T. Trefzger[177], F. Tresoldi[151], A. Tricoli[27], I.M. Trigger[163a], S. Trincaz-Duvoid[83], M.F. Tripiana[13], W. Trischuk[161], B. Trocmé[58], A. Trofymov[45], C. Troncon[94a], M. Trottier-McDonald[16], M. Trovatelli[172], L. Truong[167a,167c], M. Trzebinski[42], A. Trzupek[42], K.W. Tsang[62a], J.C-L. Tseng[122], P.V. Tsiareshka[95], G. Tsipolitis[10], N. Tsirintanis[9], S. Tsiskaridze[13], V. Tsiskaridze[51], E.G. Tskhadadze[54a], K.M. Tsui[62a], I.I. Tsukerman[99], V. Tsulaia[16], S. Tsuno[69], D. Tsybychev[150], Y. Tu[62b], A. Tudorache[28b], V. Tudorache[28b], T.T. Tulbure[28a], A.N. Tuna[59], S.A. Tupputi[22a,22b], S. Turchikhin[68], D. Turgeman[175], I. Turk Cakir[4b,au], R. Turra[94a], P.M. Tuts[38], G. Ucchielli[22a,22b], I. Ueda[69], M. Ughetto[148a,148b], F. Ukegawa[164], G. Unal[32], A. Undrus[27], G. Unel[166], F.C. Ungaro[91], Y. Unno[69], C. Unverdorben[102], J. Urban[146b], P. Urquijo[91], P. Urrejola[86], G. Usai[8], J. Usui[69], L. Vacavant[88], V. Vacek[130], B. Vachon[90], C. Valderanis[102], E. Valdes Santurio[148a,148b], S. Valentinetti[22a,22b], A. Valero[170], L. Valéry[13], S. Valkar[131], A. Vallier[5], J.A. Valls Ferrer[170], W. Van Den Wollenberg[109], H. van der Graaf[109], N. van Eldik[154], P. van Gemmeren[6], J. Van Nieuwkoop[144], I. van Vulpen[109], M.C. van Woerden[109], M. Vanadia[135a,135b], W. Vandelli[32], R. Vanguri[124], A. Vaniachine[160], P. Vankov[109], G. Vardanyan[180], R. Vari[134a], E.W. Varnes[7], C. Varni[53a,53b], T. Varol[43], D. Varouchas[119], A. Vartapetian[8], K.E. Varvell[152], J.G. Vasquez[179], G.A. Vasquez[34b], F. Vazeille[37], T. Vazquez Schroeder[90], J. Veatch[57], V. Veeraraghavan[7], L.M. Veloce[161], F. Veloso[128a,128c], S. Veneziano[134a], A. Ventura[76a,76b], M. Venturi[172], N. Venturi[161], A. Venturini[25], V. Vercesi[123a], M. Verducci[136a,136b], W. Verkerke[109], J.C. Vermeulen[109], M.C. Vetterli[144,d], N. Viaux Maira[34b], O. Viazlo[84], I. Vichou[169,*], T. Vickey[141], O.E. Vickey Boeriu[141], G.H.A. Viehhauser[122], S. Viel[16], L. Vigani[122], M. Villa[22a,22b], M. Villaplana Perez[94a,94b], E. Vilucchi[50], M.G. Vincter[31], V.B. Vinogradov[68], A. Vishwakarma[45], C. Vittori[22a,22b], I. Vivarelli[151], S. Vlachos[10], M. Vlasak[130], M. Vogel[178], P. Vokac[130], G. Volpi[126a,126b], H. von der Schmitt[103], E. von Toerne[23], V. Vorobel[131], K. Vorobev[100], M. Vos[170], R. Voss[32], J.H. Vossebeld[77], N. Vranjes[14], M. Vranjes Milosavljevic[14], V. Vrba[130], M. Vreeswijk[109], R. Vuillermet[32], I. Vukotic[33], P. Wagner[23], W. Wagner[178], J. Wagner-Kuhr[102], H. Wahlberg[74], S. Wahrmund[47], J. Wakabayashi[105], J. Walder[75], R. Walker[102], W. Walkowiak[143], V. Wallangen[148a,148b], C. Wang[35b], C. Wang[36b,av], F. Wang[176], H. Wang[16], H. Wang[3], J. Wang[45], J. Wang[152], Q. Wang[115], R. Wang[6], S.M. Wang[153], T. Wang[38], W. Wang[153,aw], W. Wang[36a], Z. Wang[36c], C. Wanotayaroj[118], A. Warburton[90], C.P. Ward[30], D.R. Wardrope[81], A. Washbrook[49],



JHEP07(2017)107

P.M. Watkins[19], A.T. Watson[19], M.F. Watson[19], G. Watts[140], S. Watts[87], B.M. Waugh[81], A.F. Webb[11], S. Webb[86], M.S. Weber[18], S.W. Weber[177], S.A. Weber[31], J.S. Webster[6], A.R. Weidberg[122], B. Weinert[64], J. Weingarten[57], C. Weiser[51], H. Weits[109], P.S. Wells[32], T. Wenaus[27], T. Wengler[32], S. Wenig[32], N. Wermes[23], M.D. Werner[67], P. Werner[32], M. Wessels[60a], K. Whalen[118], N.L. Whallon[140], A.M. Wharton[75], A. White[8], M.J. White[1], R. White[34b], D. Whiteson[166], F.J. Wickens[133], W. Wiedenmann[176], M. Wielers[133], C. Wiglesworth[39], L.A.M. Wiik-Fuchs[23], A. Wildauer[103], F. Wilk[87], H.G. Wilkens[32], H.H. Williams[124], S. Williams[109], C. Willis[93], S. Willocq[89], J.A. Wilson[19], I. Wingerter-Seez[5], E. Winkels[151], F. Winklmeier[118], O.J. Winston[151], B.T. Winter[23], M. Wittgen[145], M. Wobisch[82,u], T.M.H. Wolf[109], R. Wolff[88], M.W. Wolter[42], H. Wolters[128a,128c], V.W.S. Wong[171], S.D. Worm[19], B.K. Wosiek[42], J. Wotschack[32], K.W. Wozniak[42], M. Wu[33], S.L. Wu[176], X. Wu[52], Y. Wu[92], T.R. Wyatt[87], B.M. Wynne[49], S. Xella[39], Z. Xi[92], L. Xia[35c], D. Xu[35a], L. Xu[27], B. Yabsley[152], S. Yacoob[147a], D. Yamaguchi[159], Y. Yamaguchi[120], A. Yamamoto[69], S. Yamamoto[157], T. Yamanaka[157], K. Yamauchi[105], Y. Yamazaki[70], Z. Yan[24], H. Yang[36c], H. Yang[16], Y. Yang[153], Z. Yang[15], W-M. Yao[16], Y.C. Yap[83], Y. Yasu[69], E. Yatsenko[5], K.H. Yau Wong[23], J. Ye[43], S. Ye[27], I. Yeletskikh[68], E. Yigitbasi[24], E. Yildirim[86], K. Yorita[174], K. Yoshihara[124], C. Young[145], C.J.S. Young[32], D.R. Yu[16], J. Yu[8], J. Yu[67], S.P.Y. Yuen[23], I. Yusuff[30,ax], B. Zabinski[42], G. Zacharis[10], R. Zaidan[13], A.M. Zaitsev[132,ak], N. Zakharchuk[45], J. Zalieckas[15], A. Zaman[150], S. Zambito[59], D. Zanzi[91], C. Zeitnitz[178], M. Zeman[130], A. Zemla[41a], J.C. Zeng[169], Q. Zeng[145], O. Zenin[132], T. Ženiš[146a], D. Zerwas[119], D. Zhang[92], F. Zhang[176], G. Zhang[36a,aq], H. Zhang[35b], J. Zhang[6], L. Zhang[51], L. Zhang[36a], M. Zhang[169], R. Zhang[23], R. Zhang[36a,av], X. Zhang[36b], Y. Zhang[35a], Z. Zhang[119], X. Zhao[43], Y. Zhao[36b,ay], Z. Zhao[36a], A. Zhemchugov[68], J. Zhong[122], B. Zhou[92], C. Zhou[176], L. Zhou[43], M. Zhou[35a], M. Zhou[150], N. Zhou[35c], C.G. Zhu[36b], H. Zhu[35a], J. Zhu[92], Y. Zhu[36a], X. Zhuang[35a], K. Zhukov[98], A. Zibell[177], D. Zieminska[64], N.I. Zimine[68], C. Zimmermann[86], S. Zimmermann[51], Z. Zinonos[103], M. Zinser[86], M. Ziolkowski[143], L. Živković[14], G. Zobernig[176], A. Zoccoli[22a,22b], R. Zou[33], M. zur Nedden[17], L. Zwalinski[32].

[1] *Department of Physics, University of Adelaide, Adelaide, Australia*
[2] *Physics Department, SUNY Albany, Albany NY, U.S.A.*
[3] *Department of Physics, University of Alberta, Edmonton AB, Canada*
[4] [(a)] *Department of Physics, Ankara University, Ankara;* [(b)] *Istanbul Aydin University, Istanbul;* [(c)] *Division of Physics, TOBB University of Economics and Technology, Ankara, Turkey*
[5] *LAPP, CNRS/IN2P3 and Université Savoie Mont Blanc, Annecy-le-Vieux, France*
[6] *High Energy Physics Division, Argonne National Laboratory, Argonne IL, U.S.A.*
[7] *Department of Physics, University of Arizona, Tucson AZ, U.S.A.*
[8] *Department of Physics, The University of Texas at Arlington, Arlington TX, U.S.A.*
[9] *Physics Department, National and Kapodistrian University of Athens, Athens, Greece*
[10] *Physics Department, National Technical University of Athens, Zografou, Greece*
[11] *Department of Physics, The University of Texas at Austin, Austin TX, U.S.A.*
[12] *Institute of Physics, Azerbaijan Academy of Sciences, Baku, Azerbaijan*
[13] *Institut de Física d'Altes Energies (IFAE), The Barcelona Institute of Science and Technology, Barcelona, Spain*
[14] *Institute of Physics, University of Belgrade, Belgrade, Serbia*
[15] *Department for Physics and Technology, University of Bergen, Bergen, Norway*
[16] *Physics Division, Lawrence Berkeley National Laboratory and University of California, Berkeley CA, U.S.A.*
[17] *Department of Physics, Humboldt University, Berlin, Germany*
[18] *Albert Einstein Center for Fundamental Physics and Laboratory for High Energy Physics, University of Bern, Bern, Switzerland*



JHEP07(2017)107

[19] School of Physics and Astronomy, University of Birmingham, Birmingham, U.K.
[20] [(a)] Department of Physics, Bogazici University, Istanbul; [(b)] Department of Physics Engineering, Gaziantep University, Gaziantep; [(d)] Istanbul Bilgi University, Faculty of Engineering and Natural Sciences, Istanbul; [(e)] Bahcesehir University, Faculty of Engineering and Natural Sciences, Istanbul, Turkey
[21] Centro de Investigaciones, Universidad Antonio Narino, Bogota, Colombia
[22] [(a)] INFN Sezione di Bologna; [(b)] Dipartimento di Fisica e Astronomia, Università di Bologna, Bologna, Italy
[23] Physikalisches Institut, University of Bonn, Bonn, Germany
[24] Department of Physics, Boston University, Boston MA, U.S.A.
[25] Department of Physics, Brandeis University, Waltham MA, U.S.A.
[26] [(a)] Universidade Federal do Rio De Janeiro COPPE/EE/IF, Rio de Janeiro; [(b)] Electrical Circuits Department, Federal University of Juiz de Fora (UFJF), Juiz de Fora; [(c)] Federal University of Sao Joao del Rei (UFSJ), Sao Joao del Rei; [(d)] Instituto de Fisica, Universidade de Sao Paulo, Sao Paulo, Brazil
[27] Physics Department, Brookhaven National Laboratory, Upton NY, U.S.A.
[28] [(a)] Transilvania University of Brasov, Brasov; [(b)] Horia Hulubei National Institute of Physics and Nuclear Engineering, Bucharest; [(c)] Department of Physics, Alexandru Ioan Cuza University of Iasi, Iasi; [(d)] National Institute for Research and Development of Isotopic and Molecular Technologies, Physics Department, Cluj Napoca; [(e)] University Politehnica Bucharest, Bucharest; [(f)] West University in Timisoara, Timisoara, Romania
[29] Departamento de Física, Universidad de Buenos Aires, Buenos Aires, Argentina
[30] Cavendish Laboratory, University of Cambridge, Cambridge, U.K.
[31] Department of Physics, Carleton University, Ottawa ON, Canada
[32] CERN, Geneva, Switzerland
[33] Enrico Fermi Institute, University of Chicago, Chicago IL, U.S.A.
[34] [(a)] Departamento de Física, Pontificia Universidad Católica de Chile, Santiago; [(b)] Departamento de Física, Universidad Técnica Federico Santa María, Valparaíso, Chile
[35] [(a)] Institute of High Energy Physics, Chinese Academy of Sciences, Beijing; [(b)] Department of Physics, Nanjing University, Jiangsu; [(c)] Physics Department, Tsinghua University, Beijing 100084, China
[36] [(a)] Department of Modern Physics and State Key Laboratory of Particle Detection and Electronics, University of Science and Technology of China, Anhui; [(b)] School of Physics, Shandong University, Shandong; [(c)] Department of Physics and Astronomy, Key Laboratory for Particle Physics, Astrophysics and Cosmology, Ministry of Education; Shanghai Key Laboratory for Particle Physics and Cosmology, Shanghai Jiao Tong University, Shanghai(also at PKU-CHEP);, China
[37] Université Clermont Auvergne, CNRS/IN2P3, LPC, Clermont-Ferrand, France
[38] Nevis Laboratory, Columbia University, Irvington NY, U.S.A.
[39] Niels Bohr Institute, University of Copenhagen, Kobenhavn, Denmark
[40] [(a)] INFN Gruppo Collegato di Cosenza, Laboratori Nazionali di Frascati; [(b)] Dipartimento di Fisica, Università della Calabria, Rende, Italy
[41] [(a)] AGH University of Science and Technology, Faculty of Physics and Applied Computer Science, Krakow; [(b)] Marian Smoluchowski Institute of Physics, Jagiellonian University, Krakow, Poland
[42] Institute of Nuclear Physics Polish Academy of Sciences, Krakow, Poland
[43] Physics Department, Southern Methodist University, Dallas TX, U.S.A.
[44] Physics Department, University of Texas at Dallas, Richardson TX, U.S.A.
[45] DESY, Hamburg and Zeuthen, Germany
[46] Lehrstuhl für Experimentelle Physik IV, Technische Universität Dortmund, Dortmund, Germany
[47] Institut für Kern- und Teilchenphysik, Technische Universität Dresden, Dresden, Germany
[48] Department of Physics, Duke University, Durham NC, U.S.A.
[49] SUPA - School of Physics and Astronomy, University of Edinburgh, Edinburgh, U.K.
[50] INFN e Laboratori Nazionali di Frascati, Frascati, Italy

JHEP07(2017)107

[51] Fakultät für Mathematik und Physik, Albert-Ludwigs-Universität, Freiburg, Germany
[52] Departement de Physique Nucleaire et Corpusculaire, Université de Genève, Geneva, Switzerland
[53] [(a)] INFN Sezione di Genova; [(b)] Dipartimento di Fisica, Università di Genova, Genova, Italy
[54] [(a)] E. Andronikashvili Institute of Physics, Iv. Javakhishvili Tbilisi State University, Tbilisi; [(b)] High Energy Physics Institute, Tbilisi State University, Tbilisi, Georgia
[55] II Physikalisches Institut, Justus-Liebig-Universität Giessen, Giessen, Germany
[56] SUPA - School of Physics and Astronomy, University of Glasgow, Glasgow, U.K.
[57] II Physikalisches Institut, Georg-August-Universität, Göttingen, Germany
[58] Laboratoire de Physique Subatomique et de Cosmologie, Université Grenoble-Alpes, CNRS/IN2P3, Grenoble, France
[59] Laboratory for Particle Physics and Cosmology, Harvard University, Cambridge MA, U.S.A.
[60] [(a)] Kirchhoff-Institut für Physik, Ruprecht-Karls-Universität Heidelberg, Heidelberg; [(b)] Physikalisches Institut, Ruprecht-Karls-Universität Heidelberg, Heidelberg; [(c)] ZITI Institut für technische Informatik, Ruprecht-Karls-Universität Heidelberg, Mannheim, Germany
[61] Faculty of Applied Information Science, Hiroshima Institute of Technology, Hiroshima, Japan
[62] [(a)] Department of Physics, The Chinese University of Hong Kong, Shatin, N.T., Hong Kong; [(b)] Department of Physics, The University of Hong Kong, Hong Kong; [(c)] Department of Physics and Institute for Advanced Study, The Hong Kong University of Science and Technology, Clear Water Bay, Kowloon, Hong Kong, China
[63] Department of Physics, National Tsing Hua University, Taiwan, Taiwan
[64] Department of Physics, Indiana University, Bloomington IN, U.S.A.
[65] Institut für Astro- und Teilchenphysik, Leopold-Franzens-Universität, Innsbruck, Austria
[66] University of Iowa, Iowa City IA, U.S.A.
[67] Department of Physics and Astronomy, Iowa State University, Ames IA, U.S.A.
[68] Joint Institute for Nuclear Research, JINR Dubna, Dubna, Russia
[69] KEK, High Energy Accelerator Research Organization, Tsukuba, Japan
[70] Graduate School of Science, Kobe University, Kobe, Japan
[71] Faculty of Science, Kyoto University, Kyoto, Japan
[72] Kyoto University of Education, Kyoto, Japan
[73] Research Center for Advanced Particle Physics and Department of Physics, Kyushu University, Fukuoka, Japan
[74] Instituto de Física La Plata, Universidad Nacional de La Plata and CONICET, La Plata, Argentina
[75] Physics Department, Lancaster University, Lancaster, U.K.
[76] [(a)] INFN Sezione di Lecce; [(b)] Dipartimento di Matematica e Fisica, Università del Salento, Lecce, Italy
[77] Oliver Lodge Laboratory, University of Liverpool, Liverpool, U.K.
[78] Department of Experimental Particle Physics, Jožef Stefan Institute and Department of Physics, University of Ljubljana, Ljubljana, Slovenia
[79] School of Physics and Astronomy, Queen Mary University of London, London, U.K.
[80] Department of Physics, Royal Holloway University of London, Surrey, U.K.
[81] Department of Physics and Astronomy, University College London, London, U.K.
[82] Louisiana Tech University, Ruston LA, U.S.A.
[83] Laboratoire de Physique Nucléaire et de Hautes Energies, UPMC and Université Paris-Diderot and CNRS/IN2P3, Paris, France
[84] Fysiska institutionen, Lunds universitet, Lund, Sweden
[85] Departamento de Fisica Teorica C-15, Universidad Autonoma de Madrid, Madrid, Spain
[86] Institut für Physik, Universität Mainz, Mainz, Germany
[87] School of Physics and Astronomy, University of Manchester, Manchester, U.K.
[88] CPPM, Aix-Marseille Université and CNRS/IN2P3, Marseille, France
[89] Department of Physics, University of Massachusetts, Amherst MA, U.S.A.
[90] Department of Physics, McGill University, Montreal QC, Canada
[91] School of Physics, University of Melbourne, Victoria, Australia

JHEP07(2017)107

[92] Department of Physics, The University of Michigan, Ann Arbor MI, U.S.A.
[93] Department of Physics and Astronomy, Michigan State University, East Lansing MI, U.S.A.
[94] [(a)] INFN Sezione di Milano; [(b)] Dipartimento di Fisica, Università di Milano, Milano, Italy
[95] B.I. Stepanov Institute of Physics, National Academy of Sciences of Belarus, Minsk, Republic of Belarus
[96] Research Institute for Nuclear Problems of Byelorussian State University, Minsk, Republic of Belarus
[97] Group of Particle Physics, University of Montreal, Montreal QC, Canada
[98] P.N. Lebedev Physical Institute of the Russian Academy of Sciences, Moscow, Russia
[99] Institute for Theoretical and Experimental Physics (ITEP), Moscow, Russia
[100] National Research Nuclear University MEPhI, Moscow, Russia
[101] D.V. Skobeltsyn Institute of Nuclear Physics, M.V. Lomonosov Moscow State University, Moscow, Russia
[102] Fakultät für Physik, Ludwig-Maximilians-Universität München, München, Germany
[103] Max-Planck-Institut für Physik (Werner-Heisenberg-Institut), München, Germany
[104] Nagasaki Institute of Applied Science, Nagasaki, Japan
[105] Graduate School of Science and Kobayashi-Maskawa Institute, Nagoya University, Nagoya, Japan
[106] [(a)] INFN Sezione di Napoli; [(b)] Dipartimento di Fisica, Università di Napoli, Napoli, Italy
[107] Department of Physics and Astronomy, University of New Mexico, Albuquerque NM, U.S.A.
[108] Institute for Mathematics, Astrophysics and Particle Physics, Radboud University Nijmegen/Nikhef, Nijmegen, Netherlands
[109] Nikhef National Institute for Subatomic Physics and University of Amsterdam, Amsterdam, Netherlands
[110] Department of Physics, Northern Illinois University, DeKalb IL, U.S.A.
[111] Budker Institute of Nuclear Physics, SB RAS, Novosibirsk, Russia
[112] Department of Physics, New York University, New York NY, U.S.A.
[113] Ohio State University, Columbus OH, U.S.A.
[114] Faculty of Science, Okayama University, Okayama, Japan
[115] Homer L. Dodge Department of Physics and Astronomy, University of Oklahoma, Norman OK, U.S.A.
[116] Department of Physics, Oklahoma State University, Stillwater OK, U.S.A.
[117] Palacký University, RCPTM, Olomouc, Czech Republic
[118] Center for High Energy Physics, University of Oregon, Eugene OR, U.S.A.
[119] LAL, Univ. Paris-Sud, CNRS/IN2P3, Université Paris-Saclay, Orsay, France
[120] Graduate School of Science, Osaka University, Osaka, Japan
[121] Department of Physics, University of Oslo, Oslo, Norway
[122] Department of Physics, Oxford University, Oxford, U.K.
[123] [(a)] INFN Sezione di Pavia; [(b)] Dipartimento di Fisica, Università di Pavia, Pavia, Italy
[124] Department of Physics, University of Pennsylvania, Philadelphia PA, U.S.A.
[125] National Research Centre "Kurchatov Institute" B.P.Konstantinov Petersburg Nuclear Physics Institute, St. Petersburg, Russia
[126] [(a)] INFN Sezione di Pisa; [(b)] Dipartimento di Fisica E. Fermi, Università di Pisa, Pisa, Italy
[127] Department of Physics and Astronomy, University of Pittsburgh, Pittsburgh PA, U.S.A.
[128] [(a)] Laboratório de Instrumentação e Física Experimental de Partículas - LIP, Lisboa; [(b)] Faculdade de Ciências, Universidade de Lisboa, Lisboa; [(c)] Department of Physics, University of Coimbra, Coimbra; [(d)] Centro de Física Nuclear da Universidade de Lisboa, Lisboa; [(e)] Departamento de Fisica, Universidade do Minho, Braga; [(f)] Departamento de Fisica Teorica y del Cosmos and CAFPE, Universidad de Granada, Granada; [(g)] Dep Fisica and CEFITEC of Faculdade de Ciencias e Tecnologia, Universidade Nova de Lisboa, Caparica, Portugal
[129] Institute of Physics, Academy of Sciences of the Czech Republic, Praha, Czech Republic
[130] Czech Technical University in Prague, Praha, Czech Republic
[131] Charles University, Faculty of Mathematics and Physics, Prague, Czech Republic

JHEP07(2017)107

[132] State Research Center Institute for High Energy Physics (Protvino), NRC KI, Russia
[133] Particle Physics Department, Rutherford Appleton Laboratory, Didcot, U.K.
[134] [(a)] INFN Sezione di Roma; [(b)] Dipartimento di Fisica, Sapienza Università di Roma, Roma, Italy
[135] [(a)] INFN Sezione di Roma Tor Vergata; [(b)] Dipartimento di Fisica, Università di Roma Tor Vergata, Roma, Italy
[136] [(a)] INFN Sezione di Roma Tre; [(b)] Dipartimento di Matematica e Fisica, Università Roma Tre, Roma, Italy
[137] [(a)] Faculté des Sciences Ain Chock, Réseau Universitaire de Physique des Hautes Energies - Université Hassan II, Casablanca; [(b)] Centre National de l'Energie des Sciences Techniques Nucleaires, Rabat; [(c)] Faculté des Sciences Semlalia, Université Cadi Ayyad, LPHEA-Marrakech; [(d)] Faculté des Sciences, Université Mohamed Premier and LPTPM, Oujda; [(e)] Faculté des sciences, Université Mohammed V, Rabat, Morocco
[138] DSM/IRFU (Institut de Recherches sur les Lois Fondamentales de l'Univers), CEA Saclay (Commissariat à l'Energie Atomique et aux Energies Alternatives), Gif-sur-Yvette, France
[139] Santa Cruz Institute for Particle Physics, University of California Santa Cruz, Santa Cruz CA, U.S.A.
[140] Department of Physics, University of Washington, Seattle WA, U.S.A.
[141] Department of Physics and Astronomy, University of Sheffield, Sheffield, U.K.
[142] Department of Physics, Shinshu University, Nagano, Japan
[143] Department Physik, Universität Siegen, Siegen, Germany
[144] Department of Physics, Simon Fraser University, Burnaby BC, Canada
[145] SLAC National Accelerator Laboratory, Stanford CA, U.S.A.
[146] [(a)] Faculty of Mathematics, Physics & Informatics, Comenius University, Bratislava; [(b)] Department of Subnuclear Physics, Institute of Experimental Physics of the Slovak Academy of Sciences, Kosice, Slovak Republic
[147] [(a)] Department of Physics, University of Cape Town, Cape Town; [(b)] Department of Physics, University of Johannesburg, Johannesburg; [(c)] School of Physics, University of the Witwatersrand, Johannesburg, South Africa
[148] [(a)] Department of Physics, Stockholm University; [(b)] The Oskar Klein Centre, Stockholm, Sweden
[149] Physics Department, Royal Institute of Technology, Stockholm, Sweden
[150] Departments of Physics & Astronomy and Chemistry, Stony Brook University, Stony Brook NY, U.S.A.
[151] Department of Physics and Astronomy, University of Sussex, Brighton, U.K.
[152] School of Physics, University of Sydney, Sydney, Australia
[153] Institute of Physics, Academia Sinica, Taipei, Taiwan
[154] Department of Physics, Technion: Israel Institute of Technology, Haifa, Israel
[155] Raymond and Beverly Sackler School of Physics and Astronomy, Tel Aviv University, Tel Aviv, Israel
[156] Department of Physics, Aristotle University of Thessaloniki, Thessaloniki, Greece
[157] International Center for Elementary Particle Physics and Department of Physics, The University of Tokyo, Tokyo, Japan
[158] Graduate School of Science and Technology, Tokyo Metropolitan University, Tokyo, Japan
[159] Department of Physics, Tokyo Institute of Technology, Tokyo, Japan
[160] Tomsk State University, Tomsk, Russia
[161] Department of Physics, University of Toronto, Toronto ON, Canada
[162] [(a)] INFN-TIFPA; [(b)] University of Trento, Trento, Italy
[163] [(a)] TRIUMF, Vancouver BC; [(b)] Department of Physics and Astronomy, York University, Toronto ON, Canada
[164] Faculty of Pure and Applied Sciences, and Center for Integrated Research in Fundamental Science and Engineering, University of Tsukuba, Tsukuba, Japan
[165] Department of Physics and Astronomy, Tufts University, Medford MA, U.S.A.
[166] Department of Physics and Astronomy, University of California Irvine, Irvine CA, U.S.A.

JHEP07(2017)107

[167] [(a)] INFN Gruppo Collegato di Udine, Sezione di Trieste, Udine; [(b)] ICTP, Trieste; [(c)] Dipartimento di Chimica, Fisica e Ambiente, Università di Udine, Udine, Italy
[168] Department of Physics and Astronomy, University of Uppsala, Uppsala, Sweden
[169] Department of Physics, University of Illinois, Urbana IL, U.S.A.
[170] Instituto de Fisica Corpuscular (IFIC), Centro Mixto Universidad de Valencia - CSIC, Spain
[171] Department of Physics, University of British Columbia, Vancouver BC, Canada
[172] Department of Physics and Astronomy, University of Victoria, Victoria BC, Canada
[173] Department of Physics, University of Warwick, Coventry, U.K.
[174] Waseda University, Tokyo, Japan
[175] Department of Particle Physics, The Weizmann Institute of Science, Rehovot, Israel
[176] Department of Physics, University of Wisconsin, Madison WI, U.S.A.
[177] Fakultät für Physik und Astronomie, Julius-Maximilians-Universität, Würzburg, Germany
[178] Fakultät für Mathematik und Naturwissenschaften, Fachgruppe Physik, Bergische Universität Wuppertal, Wuppertal, Germany
[179] Department of Physics, Yale University, New Haven CT, U.S.A.
[180] Yerevan Physics Institute, Yerevan, Armenia
[181] CH-1211 Geneva 23, Switzerland
[182] Centre de Calcul de l'Institut National de Physique Nucléaire et de Physique des Particules (IN2P3), Villeurbanne, France

[a] Also at Department of Physics, King's College London, London, U.K.
[b] Also at Institute of Physics, Azerbaijan Academy of Sciences, Baku, Azerbaijan
[c] Also at Novosibirsk State University, Novosibirsk, Russia
[d] Also at TRIUMF, Vancouver BC, Canada
[e] Also at Department of Physics & Astronomy, University of Louisville, Louisville, KY, U.S.A.
[f] Also at Physics Department, An-Najah National University, Nablus, Palestine
[g] Also at Department of Physics, California State University, Fresno CA, U.S.A.
[h] Also at Department of Physics, University of Fribourg, Fribourg, Switzerland
[i] Also at II Physikalisches Institut, Georg-August-Universität, Göttingen, Germany
[j] Also at Departament de Fisica de la Universitat Autonoma de Barcelona, Barcelona, Spain
[k] Also at Departamento de Fisica e Astronomia, Faculdade de Ciencias, Universidade do Porto, Portugal
[l] Also at Tomsk State University, Tomsk, Russia
[m] Also at The Collaborative Innovation Center of Quantum Matter (CICQM), Beijing, China
[n] Also at Universita di Napoli Parthenope, Napoli, Italy
[o] Also at Institute of Particle Physics (IPP), Canada
[p] Also at Horia Hulubei National Institute of Physics and Nuclear Engineering, Bucharest, Romania
[q] Also at Department of Physics, St. Petersburg State Polytechnical University, St. Petersburg, Russia
[r] Also at Borough of Manhattan Community College, City University of New York, New York City, U.S.A.
[s] Also at Department of Physics, The University of Michigan, Ann Arbor MI, U.S.A.
[t] Also at Centre for High Performance Computing, CSIR Campus, Rosebank, Cape Town, South Africa
[u] Also at Louisiana Tech University, Ruston LA, U.S.A.
[v] Also at Institucio Catalana de Recerca i Estudis Avancats, ICREA, Barcelona, Spain
[w] Also at Graduate School of Science, Osaka University, Osaka, Japan
[x] Also at Fakultät für Mathematik und Physik, Albert-Ludwigs-Universität, Freiburg, Germany
[y] Also at Institute for Mathematics, Astrophysics and Particle Physics, Radboud University Nijmegen/Nikhef, Nijmegen, Netherlands
[z] Also at Department of Physics, The University of Texas at Austin, Austin TX, U.S.A.
[aa] Also at Institute of Theoretical Physics, Ilia State University, Tbilisi, Georgia

JHEP07(2017)107

[ab] Also at CERN, Geneva, Switzerland
[ac] Also at Georgian Technical University (GTU),Tbilisi, Georgia
[ad] Also at Ochadai Academic Production, Ochanomizu University, Tokyo, Japan
[ae] Also at Manhattan College, New York NY, U.S.A.
[af] Also at Departamento de Física, Pontificia Universidad Católica de Chile, Santiago, Chile
[ag] Also at Academia Sinica Grid Computing, Institute of Physics, Academia Sinica, Taipei, Taiwan
[ah] Also at School of Physics, Shandong University, Shandong, China
[ai] Also at Departamento de Fisica Teorica y del Cosmos and CAFPE, Universidad de Granada, Granada, Portugal
[aj] Also at Department of Physics, California State University, Sacramento CA, U.S.A.
[ak] Also at Moscow Institute of Physics and Technology State University, Dolgoprudny, Russia
[al] Also at Departement de Physique Nucleaire et Corpusculaire, Université de Genève, Geneva, Switzerland
[am] Also at Institut de Física d'Altes Energies (IFAE), The Barcelona Institute of Science and Technology, Barcelona, Spain
[an] Also at School of Physics, Sun Yat-sen University, Guangzhou, China
[ao] Also at Institute for Nuclear Research and Nuclear Energy (INRNE) of the Bulgarian Academy of Sciences, Sofia, Bulgaria
[ap] Also at Faculty of Physics, M.V.Lomonosov Moscow State University, Moscow, Russia
[aq] Also at Institute of Physics, Academia Sinica, Taipei, Taiwan
[ar] Also at National Research Nuclear University MEPhI, Moscow, Russia
[as] Also at Department of Physics, Stanford University, Stanford CA, U.S.A.
[at] Also at Institute for Particle and Nuclear Physics, Wigner Research Centre for Physics, Budapest, Hungary
[au] Also at Giresun University, Faculty of Engineering, Turkey
[av] Also at CPPM, Aix-Marseille Université and CNRS/IN2P3, Marseille, France
[aw] Also at Department of Physics, Nanjing University, Jiangsu, China
[ax] Also at University of Malaya, Department of Physics, Kuala Lumpur, Malaysia
[ay] Also at LAL, Univ. Paris-Sud, CNRS/IN2P3, Université Paris-Saclay, Orsay, France
[*] Deceased

JHEP07(2017)107